Comparison of Bone Marrow Mesenchymal Stem Cells from Limb and Jaw Bones

THESIS

Presented in Partial Fulfillment of the Requirements for the Degree Master of Science in the Graduate School of The Ohio State University

By

Brandon Robert Lloyd

Graduate Program in Dentistry

The Ohio State University

2016

Master's Examination Committee:

Dr. Zongyang Sun, Advisor

Dr. Susan Mallery

Dr. Hany Emam

ABSTRACT

Objectives: Bone marrow mesenchymal stem cells (BM-MSCs) from limb bones have demonstrated promises in regenerating craniofacial bones; yet little is known about the potential of BM-MSCs from craniofacial bones. This study compared BM-MSCs isolated from limb and craniofacial bones in a commonly used preclinical large animal model, the pig.

Methods: Bone marrow was aspirated from the tibia and mandible (symphysis) of 4-month-old pigs (n=4). Subsequently, BM-MSCs were isolated, expanded and confirmed by flow cytometry. To assess cell proliferation, cell doubling times were calculated from serial cell number counts over 2 weeks. Total mRNA was extracted from freshly isolated BM-MSCs and analyzed for gene expression using an Affymetrix GeneChip porcine genome array, followed by real-time RT-PCR for validation. Osteogenic capacity was assessed by quantifying alkaline phosphatase activity. Using temperature-responsive culturing plates, the abilities of BM-MSCs to form multi-layer cell sheets (for future in-vivo transplantation), along with cell viability and morphology, were evaluated by fluorescent labeling and histological staining.

Results: BM-MSCs from both locations expressed MSC markers but not hematopoietic markers. Mandibular BM-MSCs proliferated significantly faster than tibial BM-MSCs (median cell doubling times: 2.25 vs. 2.80 days, Mann-Whitney U test, $p<0.01$). Without any osteogenic induction, mandibular BM-MSC alkaline phosphatase activities were 3.3-fold (factorial ANOVA, $p<0.001$) to those of tibial BM-MSCs. Microarray analysis on one hand confirmed that overall mandibular and tibial BM-MSC gene expressions are highly correlated with each other and genes related to osteogenesis and angiogenesis were strongly expressed, and on the other hand revealed

that there were several dozen genes which were indeed differentially expressed between mandibular and tibial BM-MSCs. They include cranial neural crest-related genes *nestin* (1.23-fold) and *BMP-4* (1.79-fold), which were higher in mandibular BM-MSCs (ANOVA, $p<0.05$), a trend also confirmed by real-time RT-PCR tests. Three-layer cell sheets were successfully fabricated using both sources of BM-MSCs, but mandibular BM-MSCs required lower initial seeding density and had fewer dead cells than tibial BM-MSCs (3.13% vs. 10.25%, t-test, $p<0.05$).

Conclusions: These data indicate that mandibular BM-MSCs may possess a greater potential than limb bone BM-MSCs for craniofacial bone regeneration.

This document is dedicated to my parents Robert and Sharon who have always supported my dreams and aspirations

Acknowledgments

I would like to thank the following:

- My thesis advisor, Dr. Zongyang Sun, for his vision, guidance, and commitment to academic excellence and professionalism at the highest standard
- BoonChing Tee, for her tireless work and dedication to this project which would not have been possible without her
- My Thesis Committee members: Dr. Susan Mallery who instructed and me in the scientific process and has been a mentor for years and Dr. Hany Emam who has been continuously supportive of my research and clinical endeavors.
- Colwyn Headley, who spent extensive hours working on data collection and analysis
- The OSU orthodontic faculty for teaching me clinical wisdom
- My orthodontic co-residents for their friendship and support
- My OMFS co-residents who taught me the meaning of dedication and teamwork
- The Delta Dental Foundation for funding this project
- Sun lab grant support from:
    - AAOF Biomedical Research Award
    - NIH grant R56DE024172

Vita

June 1999	West Jordan Jr. High
2006	B.S. Biology, Utah State University
2010	D.D.S., The Ohio State University
2010-2011	Resident (PGY-1), Department of Oral & Maxillofacial Surg., University of Maryland
2013 to present	Resident, Graduate Orthodontics Program, The Ohio State University

Publications

Tong M, Lloyd B, Pei P, Mallery SR., *Human head and neck squamous cell carcinoma cells are both targets and effectors for the angiogenic cytokine, VEGF*. J Cell Biochem. 2008 Dec 1;105(5):1202-10.

Fields of Study

Major Field: Dentistry

Specialization: Orthodontics

Table of Contents

List of Tables

Table Page

List of Figures

Figure Page

CHAPTER 1

INTRODUCTION

Craniofacial Bone Defects

Deficiencies in craniofacial bone lead to noticeable cosmetic and functional limitations in many patients[1]. Oral & maxillofacial surgeons, plastic & reconstructive surgeons, and orthodontists all have a great interest in providing or restoring form/function to patients who have such defects. While some patient are born with deficiencies in bone development regionally (eg. retrogenia, maxillary/mandibular hypoplasia), other patients have complex congenital defects such as patients born with palatal clefts and those suffering from craniofacial syndromes[2]. Additionally, dentists see a large number of patients each year who suffer from localized defects in the dentoalveolar complex resulting from varied causes including: exodontia, removal of pathologic lesions such as cysts and tumors, congenital absence of teeth, and periodontal disease [3-7]. Another group of patients present each year with maxillofacial defects sustained from trauma[8]. Although the physiologic characteristics of bone provide it a strong capacity for healing after an insult [9], in such instances where the amount of bone required for repair of a defect exceeds the bone's intrinsic ability to regenerate, or in situations where the patient suffers from deficiency of bone congenitally, it becomes necessary for clinicians to develop methods to augment the reconstruction[1].

Due to its high osteogenic potential, autogenous bone grafting from other sites of the body remains the most common treatment for large bone defects[6, 10]. These grafts sometimes require vascular transfer in cases where free-flap tissue graft is necessary[11-14]. In circumstances

where more modest defects are present, however, a number of contemporary methods have been utilized. Non-vascularized cortico-cancellous autografts are frequently employed; these require a separate donor site from which the bone must be harvested[12, 15]. Allografts of different forms are also often used from banked cadaveric bone in addition to xenograft materials, generally from bovine sources[16, 17]. Local augmentation of bone by means of osteotomy advancement (eg. genioplasty advancement, bilateral sagittal split osteotomy) is commonly performed for increasing the bony prominence of portions of the face. The application of this technique, however, has limited applications due to surrounding anatomy and vital structures which could be damaged[18]. In addition to these methods, alloplastic materials have been used extensively both for facial and dentoalveolar hard tissue adaptation. Alloplastic chin implants for treatment of retrogenia are a common example of this and a variety of materials have been utilized including Mersilene®, silicone, polyamide, Medpor®, and Gor-Tex® [19]. Other examples include hydroxyapatite crystals, ceramic-based bone graft materials (eg. OsteoGraf®, ProOsteon®), and polymer-based graft materials (eg. open porosity polylactic acid polymers), which have been used in the field of dentistry[20].

Bone augmentation procedures typically cost thousands of dollars despite some variations among methods. While some methods of bone augmentation can be provided in a dental office, others require the patient to be treated in a surgical center or hospital under general anesthesia. In such situations, the cost of treatment is greatly increased[21]. In circumstances where the surgical treatment is being done for cosmetic purposes or perceived as such, medical insurance carriers may refuse to cover the cost of treatment[22, 23]. In circumstances where bone augmentation is being done as a pre-prosthetic means for dental restoration, the dental insurance carrier is typically relied upon instead of the medical insurance and the cost of such treatment often exceeds the yearly maximum payout of the patient's dental insurance provider.

Because craniofacial bone augmentation is surgical in nature, the various treatment modalities also carry with them an extensive list of risks which includes but is not limited to: pain, infection, excessive bleeding including hematoma formation, damage to nerves and surrounding structures, delayed healing, and scarring[24]. Autografts are considered a favored method of grafting because they have the basic features of an ideal bone graft, being both osteoconductive and osteoinductive[25]. Autografts, however, necessitate that bone be harvested from a separate location imparting donor site morbidity[26, 27]. The severity of this risk varies depending on the size and location of the donor site but can be substantial in cases where free tissue transfer is required[28, 29]. Negative side effects are also seen in conjunction with alloplastic materials. For instance, alloplastic chin implants have been associated with erosion of the implant into bone, migration of the implant, and capsular contracture leading to poor contour and/or unnatural appearance of the chin[2, 30]. Nerve damage can result from various grafting methods and is a concern in areas where vital structures are near osteotomy sites or in situations where the donor or recipient sites of a graft is near a neurovascular bundle. Nerve damage is also possible when bone screws are placed in bony regions that house nerve fibers[30]. The incidence of postoperative hypoesthesia or dysesthesia has been reported between 3.4-12% in cases of chin augmentation[31] but certainly the incidence of nerve damage is different for each type of surgical procedure. Some patients also experience muscle weakness in areas where surgery has been performed (eg. mentalis muscle dysfunction) which may lead to localized ptosis and facial asymmetries[30] . Furthermore, in cases where sliding osteotomies are performed, non-union or mal-union of the bony segments may occur in addition to potential infection of associated hardware, which would have to be removed[30]. In situations where allograft or xenograft materials are used, there are limitations such as possible immunogenicity and weak osteoinductivity, because these grafts have the framework of bone but lack many of the active factors of live autogenous bone[32-34]. Because of the limitations of these current methods, researchers continue to

investigate the specific cells and mechanisms involved in osseous regeneration in order to discover improved clinical methods.

Bone Marrow - Mesenchymal Stem Cells (BM-MSCs)

Histologically the bony structure of the craniofacial bones is composed of cells and extracellular matrix. The interaction of cells, their chemical products, and the bony matrix allows for regulation of remodeling and local repair[35]. Present in the cellular structure of bone are osteocytes, osteoblasts, bone-lining cells, and osteoclasts. Also stored in the marrow spaces of the craniofacial bone is an abundant collection of mesenchymal stem cells (MSCs). These cells are believed to play a role in new bone formation, or osteogenesis, but also have the potential to differentiate into other cell types including fibroblasts, chondrocytes, adipocytes, and muscle cells when induced by other cells or growth factors[35].

Recent advances in cell-based regenerative medicine have demonstrated the ability to utilize MSCs to regenerate specific tissues[36, 37]. Earlier studies including those from our lab have established that MSCs isolated from various sources can differentiate into osteoprogenitor cells[38-42]. Therefore, these unique cells demonstrate great clinical potential in that the ability to harvest, culture and differentiate multipotent bone marrow-derived mesenchymal stem cells (BM-MSCs) from a patient and transplant the cells back in the host is consistent with a biologically customized form of patient care. MSCs derived from limb and iliac bone marrow have been shown to be suitable for regenerating bone and have been the mainstay in bone regeneration studies for many years. MSCs, nevertheless, may also be isolated from craniofacial sites including the maxilla and mandible[39, 43-45]. The osteogenic characteristics of MSCs isolated from craniofacial bone marrow have been studied to a limited degree but the capacities of jaw BM-MSCs for bone regeneration is still largely unknown[39, 45]. Akintoye et al. compared MSCs

isolated from small bone pieces at third molar extraction sites to MSCs extracted from iliac crest bone marrow and Aghaloo et al. compared MSCs flushed through third molar extraction sites to tibial MSCs in rats, but so far no study has compared MSCs directly derived from mandibular bone marrow to those isolated from long bone marrow. The embryologic origin of the mesenchymal tissues in limb and jaw bones is known to be different: mesenchyme in the craniofacial region has a neural crest origin while mesenchyme from the limb is derived from lateral plate mesoderm[46]. However, whether this difference affects postnatal (or adult) MSCs from these two sources is not well understood. In fact, no study has characterized the differences in gene expression using contemporary techniques such as RNA microarray[47], between limb and craniofacial BM-MSCs.

Cell-based Tissue Engineering

Developing tissues from cells including BM-MSCs is a constantly evolving subject in science. Numerous animal studies and clinical trials have demonstrated the feasibility of transplanting *in vitro*-fabricated tissues to desired defect sites[48-52]. Regeneration and healing of tissues by direct injection of dissociated cells is a commonly used delivery technique that has been used clinically[53, 54]. However, there are limitations associated with injection of dissociated cells including difficulties in cell engrafting the target tissue and high death rate of injected cells[55, 56]. To overcome the challenges associated with direct injection of cells, scientists and clinicians have increasingly looked toward tissue engineering over the past twenty years[57]. Tissue engineering is based on the concept that three-dimensional scaffolds can be used as an alternative to extracellular matrix; where cells are seeded into the scaffolds and the proper combination of the two yields a functional substitute for missing or damaged tissue[58]. Dozens of exogenous scaffold materials have been utilized in previous studies for cellular bone tissue engineering

including some that are biodegradable and some that are not. Some of the previously utilized scaffold materials include: hydroxyapatite, tricalcium phosphate, biphasic calcium phosphate, collagen type 1, chitosan, calcium alginate, hyaluronic acid, poly(glycolic) acid and other synthetic polymers, micro- and nano-composites, and demineralized bone matrix[57]. However, using exogenous scaffolds for *in vivo* cell transplantation has its own drawbacks, such as needing a surgical approach to deliver, potential immune response including elevated inflammatory reactions by the host to foreign materials, fluctuating degradation rate, and poor cell-attachment efficiency, etc.[59].

Scaffold-Free Cell Sheets

'Cell sheet engineering' is an innovative method by which investigators have attempted to circumvent some of the disadvantages associated with exogenous scaffolds that are classically used in tissue engineering. Scaffold-free cell sheets are created by culturing cells on dishes surface-treated with a unique temperature-responsive molecule: typically poly(*N*-isopropylacrylamide) or PIPAAm. At 20 ºC, the surface of the PIPAAm-coated dish becomes hydrophilic and cells do not attach to the surface but when the temperature rises to 37 ºC, the surface become hydrophobic and cells readily attach and can proliferate on the surface[60]. This method of culturing cells was developed over two decades ago[61, 62] and has become increasingly utilized in recent years[63-65]. This progressive cell culturing method obviates one of the previous challenges in tissue engineering where *in vitro*-cultured cells required detachment with proteolytic enzymes such as trypsin or dipase in order to transfer the cells after proliferating to confluence[66]. The use of such enzymes presented a challenge in tissue engineering because they disrupt the micro-intercellular junction and extracellular matrix created by the cells in culture[67]. Previous studies have reported the culture and transplantation of BM-MSC cell sheets for bone

regeneration with and without exogenous scaffolds[65, 68, 69]. Currently, however, no studies have demonstrated the efficacy of forming such sheets from craniofacial-derived BM-MSCs, or compared the efficacy of forming multi-layer cell sheets from these cells in relation to the more commonly used BM-MSCs from limb marrow.

Pig Model

This research study was developed with consideration to future live animal experimentation through which our data may find use for *in vivo* application. The pig is an ideal model for initial studies exploring human therapeutic applications because it is immunologically and physiologically more similar to humans than other non-primate species[70, 71]. A number of previous studies have incorporated the pig as a large animal pre-clinical model in craniofacial studies because the pig mandible has notable similarities to the human mandible[72-74]. Our lab previously demonstrated the ability to extract porcine BM-MSCs and transplant them back in the host for bone regeneration in a distraction osteogenesis model[38]. Accordingly, this study investigates the differences in porcine BM-MSCs derived from the tibia and mandible and compares the BM-MSCs potentials in several ways.

Specific Aims:

1. Examine the feasibility of direct bone marrow aspiration from pig mandibles and confirm mesenchymal stem cell identity of the isolated cells.
2. Compare proliferation and osteogenic capacity between mandibular and tibial BM-MSCs
3. Compare gene expression profiles between mandibular and tibial BM-MSCs.

4. Compare the efficiency in forming multi-layer scaffold-free cell sheets between mandibular and tibial BM-MSCs.

Hypotheses:

1. Bone marrow can be aspirated from pig mandibular symphyseal area and mesenchymal stem cells can be isolated from the aspirated bone marrow.
2. Porcine mandibular BM-MSCs have a stronger proliferative and osteogenic capacity than tibial BM-MSCs.
3. Porcine mandibular BM-MSCs have a different gene expression profile than tibial BM-MSCs. Particularly for cranial neural crest-related genes, mandibular BM-MSCs may express more strongly.
4. Porcine mandibular BM-MSCs have a stronger capacity in forming multi-layer scaffold-free cell sheets than tibial BM-MSCs.

CHAPTER 2

MATERIALS AND METHODS

Specimens

Bone marrow samples were obtained from four (4) domestic pigs (*Sus scrofa*) at an age (approximately 4 months) comparable to pre-teen humans in craniofacial skeletal maturity. The pigs were approximately 100 lbs in weight and were utilized by university medical students for training of endoscopic abdominal surgery immediately before bone marrow aspiration. After the pigs were placed under general anesthesia (6 mg/kg Telazol, IM; maintained by 2-3% isofluorane with 2-5% oxygen through a endotracheal intubation), bone marrow aspirates were obtained from both the mandible and the tibia using a 16-gauge aspiration needle attached to a 10 mL syringe containing 1 mL heparin (1000 U/ml). The location for bone marrow aspiration from the mandible was at the labial symphyseal area, approximately 1 cm distal to the symphyseal midline and 1 cm above the inferior symphyseal border (Fig. 1). This was the first time bone marrow was aspirated directly from the pig mandibles. This location was chosen because histologically, this area has abundant subcortical marrow space and does not contain any tooth buds. The location for bone marrow aspiration from the tibia was at the medial aspect of the proximal end, slightly distal to the tibial tuberosity. This location was recommended by Sinclair Bio-resources (Swindle MM, 2009, Sample collection series: Bone Marrow Access in Swine, Sinclair Bio-resources, Columbia, MO.).

Bone marrow was characterized by a thick, grainy appearance of aspirated fluid which was collected into the syringe along with blood which was obtained simultaneously and

accounted for approximately half of the total volume. Aspirated volumes from the mandible ranged from 10-18 mL of bone marrow-blood-heparin mixture per site and tibia aspirations ranged from 20-30 mL. Following bone marrow aspiration, with general anesthesia maintained, the animals were euthanized using 125 mg/mL KCl intravenously dosed at 0.5 mg/kg.

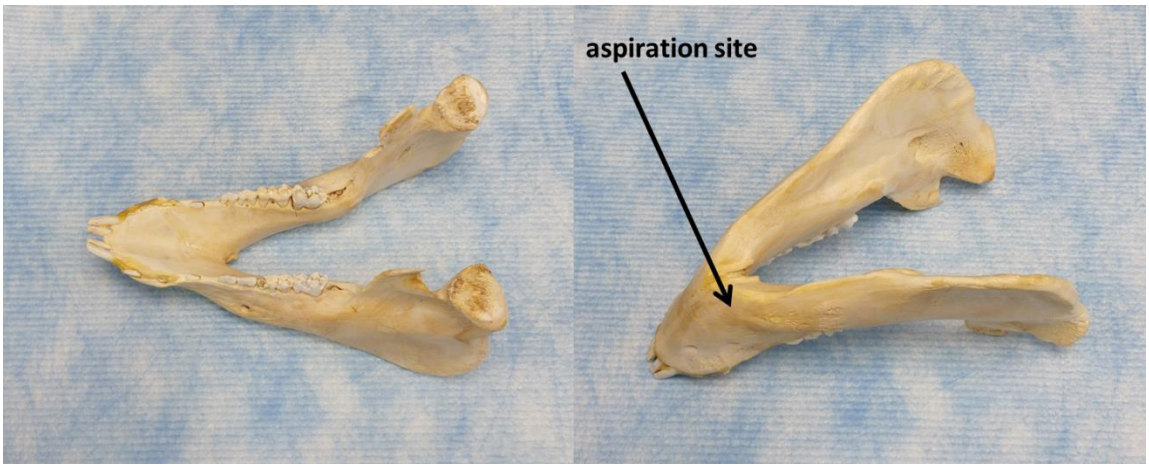

Figure 1. Location of mandibular bone marrow aspiration

Isolation and Culture of BM-MSCs

Following aspiration, bone marrow samples were processed in the laboratory using a technique adapted from an established method for human postnatal skeletal MSCs[75]. Each aspirate was combined with alpha-minimum essential medium (α-MEM, Life Technologies, Carlsbad, CA) and then centrifuged. The pellet was re-suspended in growth media (GM) that consisted of α-MEM supplemented with 20% heat-inactivated fetal bovine serum (FBS), 1% penicillin-streptomycin, and 1% L-glutamine. All culture supplements were from Life Technologies (Carlsbad, CA) unless stated otherwise. The suspension was passed through a 16 gauge needle twice and then through a cell strainer (70 μm, BD Biosciences, Bedford, MA) to obtain a single cell suspension. The mixture was then plated in flasks to incubate at 37 ºC with 5% CO_2. On day 4 after aspiration, cell cultures were washed with Dulbecco's phosphate buffered saline (D-PBS, Life Technologies, Carlsbad, CA) and provided with fresh media. Fresh media was replaced every 3-4 days until the culture reached 70-80% confluence, at which time the cells were passaged using TrypLE™ (Life Technologies, Carlsbad, CA) to dissociate the cells from the flasks.

Flow Cytometry

Phenotypic surface markers were analyzed on cultures from both tibia and mandible-derived BM-MSCs (passage 4). Two million cells from each culture were suspended in FACS buffer containing cold D-PBS supplemented with 10% FBS, 1% penicillin/streptomycin, and 1% sodium azide and then divided into 200,000 cell samples for staining/analysis. Unstained tibia and mandible cell samples were used as negative controls. Samples from each site were then stained with the following fluorescent-conjugated monoclonal antibodies specific for mesenchymal stem cell markers: phycoerythrin (PE) anti-CD105 (Acris Antibodies Inc, San Diego, CA), peridinin chlorophyll protein-cyanine (PerCP) anti-CD44 (Biolegend, San Diego,

CA), and fluorescein isothiocyanate (FITC-A) anti-CD90 (Biolegend, San Diego, CA). Corresponding cell samples were also stained with the following antibodies specific for hematopoietic cell markers: allophycocyanin (APC) anti-CD11b (Biolegend, San Diego, CA) and PE anti-CD45 (AbD Serotec, Raleigh, NC). Staining occurred in the dark for 45 minutes at 4 Cº. Expression of markers was accessed using BD LSR II flow cytometer system (BD Biosciences) and FlowJo software (Tree Star, Inc., Ashland, OR). At least 10,000 events were counted for each sample.

Cell Proliferation

Mandible and tibia-derived BM-MSCs were seeded on 12-well tissue culture-treated plates (Corning, NY) at 5,000 cells per well and resuspended in growth media. Cultures were then incubated at 37 ºC and 5% CO_2 and designated for harvest according to pre-determined time points. Cells were then detached using TrypLE™ (Life Technologies, Carlsbad, CA, USA) dissociation reagent every two days for two weeks and enumerated using a hemacytometer to record the final cell number. Triplicate measurements of each time point were used and two measurements were made of each sample to minimize measurement error. Remaining wells were fed with fresh growth media every two days until the time point at which they were designated for enumeration. The population doubling time for each culture was then calculated based on the longitudinal cell counting values up to 13 days by using an online calculator (Roth) (available from http://www.doubling-time.com/compute_more.php) which uses a least squares fitting exponential regression (Eric. W. Weisstein, From MathWorld – A Wolfram Web Resource. http://mathworld.wolfram.com/LeastSquaresFittingExponential.html.)

RNA Isolation

RNA extraction was performed on passage 0 cells cultured in growth media from both mandible and tibia-derived BM-MSCs isolated from three pigs. After rinsing twice with D-PBS,

the cells were detached from the flask using TrypLE™ (Life Technologies, Carlsbad, CA, USA). After inactivating trypsin with growth media containing FBS, the cells were centrifuged and counted. One million cells were separated from each culture and were again centrifuged directly afterward so that the media could be aspirated. RNA extraction was performed using the RNeasy Mini Kit according to the manufacturer's protocol (Qiagen, Valencia, CA). The concentration of total RNA was then quantified for each sample by Nanodrop ND-1000 (Thermo Scientific, Wilmington, DE) according to the manufacturer protocol. RNA quality was also evaluated by assessing the 260/280 and 260/230 ratios on the same machine.

Microarray Assay

A total of 3 pairs of RNA samples extracted from passage 0 tibia and mandible BM-MSC cultures of three pigs were used for this assay. Ten micrograms of RNA per sample was submitted to The Ohio State University Genomics (Microarray) Shared Resource department. The quality of total RNA was confirmed using an Agilent 2100 Bioanalyzer (Agilent Technologies, Palo Alto, CA) to ensure an RNA integrity number (RIN) above 9. Subsequently, double-stranded cDNA was generated from total RNA, labeled and fragmented with the GeneChip WT Plus reagent kit (Affymetrix, Santa Clara, CA), then hybridized to the Affymetrix GeneChip® Porcine Genome Array (Santa Clara, CA) which contains 23,937 probe sets to evaluate 20,201 genes. The array was scanned with the GeneChip Scanner 3000, normalized using the RMA algorithm in the Expression Console, and analyzed with the Transcriptome Analysis Console 2.0 (TAC 2.0) (Affymetrix).

Analyzed data collected from TAC 2.0 was sorted for Tukey's bi-weight average signals (log2) to obtain the highly abundant transcriptomes, which have a cut-off point of 10.57, 75% of the highest gene expression of 14.09. Same set of data was then sorted to obtain the differentially expressed genes, which was characterized by the ANOVA p-value < 0.05. Fold-change of 1.5 was chosen as the cut-off point since it is the point where the two cells were separated into 2

individual hierarchical clusters (Fig. 8). The gene symbols were converted to Entrez Gene ID using the Gene Accession Conversion Tool from Database for Annotation, Visualization, and Integrated Discovery (DAVID) v. 6.7. During this process, the corresponding Entrez Gene ID was chosen based on the hierarchy of the species. Specifically, ID corresponding to *homo sapiens* was first chosen, and when *homo sapiens* was absent, s*us scrofa* was prioritized, followed by *mus musculus*. Subsequently, any duplicates and uncharacterized proteins were eliminated, while the unrecognized genes with names ended with "-like" were matched to their human homologs in Uniprot.org. Functional annotation was performed on the highly abundant transcriptomes and differentially expressed genes using the clustering tool in DAVID. Finally, the microarray data will be deposited in the NCBI Gene Expression Omnibus prior to manuscript publication.

Reverse-transcription Real-time Polymerase Chain Reaction (RT-PCR):

Isolated RNA samples (3 pairs) as mentioned above were used for this test. Briefly, for each RNA sample, 1 µg of total RNA was reverse transcribed to cDNA using the SuperScript III First-Strand Synthesis System for RT-PCR kit according to the manufacturer's protocol (Invitrogen, Life Technologies, Grand Island, NY). The samples were kept on ice throughout the procedure, except during pipetting and during MasterCyler (Eppendorf®, Foster City, USA) application. Resultant cDNA was diluted 1:1 using 30 µl of sterile water and stored at -20 ºC until all samples were prepared for real-time PCR assay.

Real-time PCR assay was conducted to assess the mRNA expression of two neural crest-associated genes, *BMP-4* and *Nestin*. Forward/reverse primer sets were designed using Primer-BLAST (NCBI, Bethesda, MD) for *Nestin* (fragment size 94 base pair (bp); forward, 5'-TCTCTCAGCATCTTGGACCCTA -3'; reverse, 3'- TAGGACTCAGGACAGAGAGCAA -5') and housekeeping gene *β–actin* (fragment size 179 bp; forward, 5'-TCCCTGGAGAAGAGCTACGA-3', reverse, 5'- TAGAGGTCCTTGCGGATGTC-3'). The primer set for porcine neural crest-related protein *BMP-4* was commercially available from

Qiagen (RT² qPCR Primer Assay for Pig BMP4, Product 330001, Qiagen, Valencia, CA). These primer sets were tested for efficacy along with a primer set for known house-keeping gene *β-actin*. The scouting trial demonstrated that the BMP-4 primer set and one of the *Nestin* primer sets were sufficiently efficacious to detect levels of the associated gene transcripts (see Table 1). These primers were subsequently used for the PCR assay. In order to detect the expression of *BMP-4* and *Nestin*, real-time PCR was performed using iQ-SYBR Green Supermix (Bio-Rad, Hercules, CA) and the iCycler (Bio-Rad, Hercules, CA) according to the manufacturer's protocols. Duplicate trials were completed for each cDNA sample.

For each of the genes investigated, the expression was calculated using the comparative C_T method (or $2^{-\Delta\Delta Ct}$ method). Briefly, the CT values of PCR sample duplicates were averaged and normalized to *β-actin*, which derived ΔCt. The average ΔCt value obtained from the PCR reaction of each mandible-derived sample was further normalized to the average ΔCt value obtained from the tibia-derived sample corresponding to the same animal. Gene expression comparison was then calculated between sites (mandible vs tibia) in terms of the fold of change.

Assessment of Osteogenic Differentiation

Qualitative assessment: Individual 22 x 22 mm glass microscope coverslips were placed at the bottom of each partition of a 6-well plate (Corning Inc., Corning, NY). Tibia and mandible-derived BM-MSCs were then seeded at a density of 100,000 cells per well. Cultures were given 2 mL growth media supplemented with fibroblast growth factor 2 (FGF-2), a growth factor likely to stimulate MSC proliferation and osteogenic differentiation, at 0 ng/mL, 5 ng/mL, or 10 ng/mL. Cells were replaced with fresh corresponding media every three days and kept at 37 ºC and 5% CO_2. On day 10, cells grown on the glass slides were evaluated using the Leukocyte Alkaline Phosphatase Kit (85-L2, Sigma Aldrich®, St Louis, MO). Cells were rinsed with D-PBS and fixed with an acetone buffer consisting of citrate and acetone for thirty seconds. Cells on the glass slide were rinsed twice with tap water and then, in the dark, transferred face-up into staining

dishes which contained a light-sensitive staining mixture of distilled water, Napthol, and Fast Violet B salt (Sigma Aldrich, St Louis, MO). After 30 minutes of staining in the dark, the glass slides were rinsed in a solution of deionized water for 2 minutes and then counterstained in a hematoxylin solution for 10 minutes. Finally the cells on the glass slide were rinsed in a tap water solution for two minutes until the solution was clear.

Quantitative assessment: Similar to the qualitative assessment, tibia and mandible-derived BM-MSCs were seeded on a tissue-culture treated 6-well plate at 100,000 cells per well, and treated with fibroblast growth factor 2 (FGF-2) at 0 ng/mL, 5 ng/mL, or 10 ng/mL. Identical culture conditions were maintained as those in the qualitative assessment. On day 10, cell samples were rinsed, scraped, and then lysed using 300µL of 0.2% Triton®-X-100 solution (Fisher Scientific, Waltham, MA). The collected cells were vortexed, placed on a shaker for 20 minutes, and then frozen. The mixture was later thawed and alkaline phosphatase (ALP) activity was quantified using the QuantiChrome™ Alkaline Phosphatase Kit (BioAssay Systems, Hayward, CA) according to the manufacturer's protocol.

Muilti-layer Cell Sheet Fabrication

Culture: Mandible and tibia BM-MSC cultures were expanded from an early passage stage (2 or 3). Cells were then seeded into 12-well plates with temperature-responsive surfaces (Nunc™ dishes with UpCell™ surface, Thermo Scientific, USA) in growth media. Varying seeding densities (100K-400K/well) were attempted to compare the time needed to form a complete cell sheet between mandibular and tibia BM-MSCs. Tibia-derived cells were also grown on 24-well temperature responsive plates at densities of 300K-400K/well, a seeding density that was higher than that on the 12-well plates due to the smaller well size .

Layering: Thirty minutes prior to manipulating the cell sheets, 35mm tissue culture plates were prepared by coating the surfaces with 1mL CELLstart™ CTS™ (Life Technologies, Carlsbad, CA, USA) mixture which was obtained by adding 10µL of CELLstart™ substrate to

990μL of D-PBS supplemented with calcium chloride and magnesium chloride (Life Technologies, Carlsbad, CA). The coated dishes were then placed in the incubator (37 ºC, 5% CO_2), set apart for receiving post-detachment cell sheet layers. After 48 hours of incubation on the temperature-responsive plates, the BM-MSC-confluent UpCell™ plates were taken out from the incubator and placed under room temperature (approx. 21 ºC) for cell sheet detachment. Cell cultures demonstrating a high degree of confluence required between 15-75 minutes to detach and not all wells on the plate detached simultaneously. Detachment time varied between plates and also between wells. For trials on which adequate confluence was obtained, the resultant cell sheet was fragile but able to be manipulated physically. Intact cell sheets were manipulated using pipettes. Before transfer, CELLstart™ coated plates were removed from the incubator and brought to the culture hood where excess fluid was aspirated off with a micropipette. Both 25mL standard pipettes and 1000μL micropipettes with a cut tip were used to transfer the cell sheets from the UpCell™ surface to the CELLstart™ coated plate. After being transferred to the new plate, the cell sheet was slowly and carefully moved to the center of the dish in a manner that the cell sheet was not folded over on itself. This procedure was technique-sensitive and generally took several minutes. After the cell sheet was correctly positioned on the cell sheet, a small amount of culture media was kept to barely cover the cell sheet and the plate was returned to the incubator and allowed approximately 30 minutes to adhere. Subsequently, the plate was retrieved from the incubator with an adherent cell sheet, over which a second cell sheet detached from another temperature-responsive plate was pipetted. The resultant stacked sheets were placed back into the incubator after excess media was removed from the dish. After 30 minutes of incubation, the stacked sheets were retrieved again and a third sheet was added in the same manner. Following this, excess media was again removed for a 30 minute incubation window to allow adherence. Finally, the stacked cell sheets were replenished with 2 mL of media and allowed to incubate for 24 hours prior to assessing cell viability.

Cell viability staining: Twenty-four hours after stacking, the triple-layer BM-MSC cell sheets were washed gently with D-PBS; after which they were treated using the LIVE/DEAD® Viability Kit for mammalian cells (Molecular Probes™, Invitrogen detection technologies, Eugene, OR) according to the manufacturer's protocol. A 4 mM solution of EthD-1was created by adding 20µL of 2mM EthD-1 stock solution to 10mL of D-PBS at room temperature. Five microliters of 4 mM calcein AM stock solution was then added to the EthD-1 solution, yielding a final working mixture consisting of 2 mM calcein AM and 4mM EthD-1. Then, 100-150 µL of LIVE/DEAD® stock reagent mixture was added to the washed cells and incubated at room temperature for 30 minutes. Cell sheets were then transferred from the 35mm culture dish to a glass slide through gentle manipulation with a micropipette tip. To preserve the architecture of the cell sheets, the cell sheets were not cover-slipped. The slides were immediately observed under a fluorescence microscope (Axioplan 400 Zeiss, Carl Zeiss MicroImaging, NY) to evaluate the amount of live and dead cells.

Histologic Staining/Microscopy: Triple-layer cell sheets collected immediately after 24 hours of incubation, or immediately after the live/dead staining procedures, were fixed using a 4% paraformaldehyde solution for approximately 24 hours. After fixation, the specimens were embedded with paraffin and sectioned into 5µm-thick slices perpendicularly to the layers. The sections were subsequently stained by hematoxylin and eosin (H&E), cover-slipped and viewed under a light microscope (Olympus BX51, Olympus America Inc, Center Valley, PA) for histological features of the cells and matrices.

Statistical Analysis:

One-way ANOVA tests were used to compare tibial and mandibular BM-MSC microarray data as well as the alkaline phosphatase assay results. Pearson's tests were used to calculate the coefficient of correlation in the microarray data. For proliferation data, cell doubling

times were compared using the Mann-Whitney U test. For normally distributed data including analyses of live/dead staining of mandibular and tibial BM-MSC scaffold-free cell sheets, paired student t-tests were used. A p-value of <0.05 was considered significant for all analyses. All statistical analyses were performed using SPSS v. 20 software (IBM, Chicago, IL).

CHAPTER 3

MANUSCRIPT

Comparison of Porcine Bone Marrow Mesenchymal Stem Cells from Limb and Jaw Bones

Brandon Lloyd[1]

Boon Ching Tee[1]

Colwyn Headley[1]

Hany Emam[2]

Susan Mallery[3]

Zongyang Sun[1,*]

[1] Division of Orthodontics, College of Dentistry, The Ohio State University, Columbus, OH, USA

[2] Division of Oral and Maxillofacial Surgery, College of Dentistry, The Ohio State University, Columbus, OH, USA

[3] Division of Oral and Maxillofacial Pathology and Radiology, College of Dentistry, The Ohio State University, Columbus, OH, USA

* Corresponding author at: Division of Orthodontics, College of Dentistry, The Ohio State University, Rm 4088 Postle Hall, 305 W 12th AVE, Columbus, OH 43210, USA. Tel: 614-247-7944; Fax: 614-688-3077; Email: sun.254@osu.edu

ABSTRACT

Objective: Craniofacial bone defects caused by injuries and congenital diseases are a formidable challenge to clinicians. Research has shown promise in using bone marrow mesenchymal stem cells (BM-MSCs) from limb bones for craniofacial bone regeneration; yet little is known about the potential of BM-MSCs from craniofacial bones. This study compares BM-MSCs isolated from limb and craniofacial bones in pigs, a preclinical model closely resembling humans.

Design: Bone marrow was aspirated from the tibia and mandible of four-month-old pigs (n=4), followed by BM-MSC isolation, culture-expansion and confirmation by flow cytometry. Proliferation rates were compared using population doubling times. Osteogenic differentiation was evaluated by quantifying alkaline phosphatase (ALP) activity. Total mRNA was then extracted from freshly isolated BM-MSCs and analyzed to compare gene expressions of tibial and mandibular BM-MSCs using an Affymetrix GeneChip porcine genome array, followed by real-time RT-PCR evaluation of two neural crest markers.

Results: BM-MSCs from both locations expressed MSC markers but not hematopoietic markers. Mandibular BM-MSCs proliferated significantly faster than tibial BM-MSCs. Without osteogenic inducers, mandibular BM-MSC alkaline phosphatase activities were 3.3-fold greater than those of tibial origin. Microarray analysis identified 383 differentially expressed genes in mandibular and tibial BM-MSCs, including higher expression of cranial neural crest-related genes *nestin* and *BMP-4* in mandibular BM-MSCs, a trend also confirmed by real-time RT-PCR. Among differently expressed genes, only 47 showed greater than 1.5-fold differences in expression.

Conclusions: These data indicate that despite many similarities in gene expression, mandibular BM-MSCs express of number of genes differently than tibial BM-MSCs and have a phenotypic profile that may make them advantageous for craniofacial bone regeneration.

Keywords: marrow stromal cells, microarray, craniofacial bone regeneration, BMP-4, osteogenic

1. INTRODUCTION

Bony defects of the face and jaws may result from congenital malformations, infections, neoplastic processes, trauma, or from surgical treatment such as dental extraction. Appropriate reconstruction of these defects is functionally necessary and esthetically important, but clinically challenging. The current standard treatment approach, autogenous bone grafts, is effective to a certain degree, but often comes with donor site morbidity. The finite amount of donor bone also greatly limits its application[76].

Mesenchymal stem cell (MSC)-based tissue engineering has been studied in recent years as an alternative treatment for craniofacial defect. Although extensive research has confirmed that adult MSCs can be derived from a number of tissues (including periodontium, dental pulp, fat, etc.), bone marrow derived mesenchymal stem cells (BM-MSCs) were the first described MSCs and remain among the most reliable and relevant sources of MSCs for skeletal regeneration[40, 77, 78]. For years, the iliac crest or long bones such as the tibia and femur have been most commonly utilized to obtain BM-MSCs for craniofacial regeneration[79-85], while it remains uncertain whether BM-MSCs from craniofacial bones are more potent for this purpose. Several recent studies isolated BM-MSCs from the maxilla and mandible by rinsing fragments of bone or by flushing cells through the extraction sockets and compared their properties with those from long bones or iliac crest so far[39, 45, 86]. Briefly, in both rats[45, 86] and humans[39], craniofacial BM-MSCs indeed demonstrated greater proliferative and osteogenic capacities than BM-MSCs from long bones[45, 86] or from the iliac crest[39].

Embryonically, the development of craniofacial bones differs from that of long bones by having cranial neural crest contribution[87]. Whether this difference is retained in adult BM-MSCs and influences their regenerative potential are largely unknown. The few studies mentioned above explored differences in the expression of several genes including *Oct4*, *Nanog*, *Sox2*, *Nestin*,

Runx2, *OSX*, *OPN*, and *OCN*[86] as well as *endostatin* and *TGFβ-R2*[39], but no studies have assessed genome-wide differences between craniofacial and long bone BM-MSCs.

Previously, our lab and others showed that the pig is an outstanding model for pre-clinical craniofacial bone studies. Not only does the domestic pig have similar size and dentoalveolar function to humans, it is also understood to be physiologically and immunologically more similar to humans than other non-primate species. In this study, we used the pig to further evaluate the differences between craniofacial and long bone BM-MSCs. Not only did we assess phenotypic differences reported in other species, we further evaluated similarities and differences in the genome-wide expression profiles of these two types of MSCs using microarray technology.

2. MATERIALS AND METHODS

2.1. Pig specimens

Bone marrow samples were obtained from four (4) domestic pigs (*Sus scrofa*) at an age (approximately 4 months) comparable to pre-teen humans in craniofacial skeletal maturity. The pigs were approximately 100 lbs in weight and were utilized by university medical students for training of endoscopic abdominal surgery immediately before bone marrow aspiration. After the pigs were placed under general anesthesia (6 mg/kg Telazol, IM; maintained by 2-3% isofluorane with 2-5% oxygen through a endotracheal intubation), bone marrow aspirates were obtained from both the mandible and the tibia using a 16-gauge aspiration needle attached to a 10 mL syringe containing 1 mL heparin (1000 U/ml). The location for bone marrow aspiration from the mandible was at the labial symphyseal area, approximately 1 cm distal to the symphyseal midline and 1 cm above the inferior symphyseal border (Fig. 1). This was the first time bone marrow was aspirated directly from the pig mandibles. This location was chosen because histologically, this

area has abundant subcortical marrow space and does not contain any tooth buds. The location for bone marrow aspiration from the tibia was at the medial aspect of the proximal end, slightly distal to the tibial tuberosity. This location was recommended by Sinclair Bio-resources (Swindle MM, 2009, Sample collection series: Bone Marrow Access in Swine, Sinclair Bio-resources, Columbia, MO.).

Bone marrow was characterized by a thick, grainy appearance of aspirated fluid which was collected into the syringe along with blood which was obtained simultaneously and accounted for approximately half of the total volume. Aspirated volumes from the mandible ranged from 10-18 mL of bone marrow-blood-heparin mixture per site and tibia aspirations ranged from 20-30 mL. Following bone marrow aspiration, with general anesthesia maintained, the animals were euthanized using 125 mg/mL KCl intravenously dosed at 0.5 mg/kg.

2.2. Isolation and culture of BM-MSCs

Following aspiration, bone marrow samples were processed in the laboratory using a technique adapted from an established method for human postnatal skeletal MSCs[75]. Each aspirate was combined with alpha-minimum essential medium (α-MEM, Life Technologies, Carlsbad, CA) and then centrifuged. The pellet was re-suspended in growth media (GM) that consisted of α-MEM supplemented with 20% heat-inactivated fetal bovine serum (FBS), 1% penicillin-streptomycin, and 1% L-glutamine. All culture supplements were from Life Technologies (Carlsbad, CA) unless stated otherwise. The suspension was passed through a 16 gauge needle twice and then through a cell strainer (70 μm, BD Biosciences, Bedford, MA) to obtain a single cell suspension. The mixture was then plated in flasks to incubate at 37 ºC with 5% CO_2. On day 4 after aspiration, cell cultures were washed with Dulbecco's phosphate buffered saline (D-PBS, Life Technologies, Carlsbad, CA) and provided with fresh media. Fresh

media was replaced every 3-4 days until the culture reached 70-80% confluence, at which time the cells were passaged using TrypLE^{TM} (Life Technologies, Carlsbad, CA) to dissociate the cells from the flasks.

2.3. Flow cytometry

Phenotypic surface markers were analyzed on cultures from both tibia and mandible-derived BM-MSCs (passage 4). Two million cells from each culture were suspended in FACS buffer containing cold D-PBS supplemented with 10% FBS, 1% penicillin/streptomycin, and 1% sodium azide and then divided into 200,000 cell samples for staining/analysis. Unstained tibia and mandible cell samples were used as negative controls. Samples from each site were then stained with the following fluorescent-conjugated monoclonal antibodies specific for mesenchymal stem cell markers: phycoerythrin (PE) anti-CD105 (Acris Antibodies Inc, San Diego, CA), peridinin chlorophyll protein-cyanine (PerCP) anti-CD44 (Biolegend, San Diego, CA), and fluorescein isothiocyanate (FITC-A) anti-CD90 (Biolegend, San Diego, CA). Corresponding cell samples were also stained with the following antibodies specific for hematopoietic cell markers: allophycocyanin (APC) anti-CD11b (Biolegend, San Diego, CA) and PE anti-CD45 (AbD Serotec, Raleigh, NC). Staining occurred in the dark for 45 minutes at 4 C^{o}. Expression of markers was accessed using BD LSR II flow cytometer system (BD Biosciences) and FlowJo software (Tree Star, Inc., Ashland, OR). At least 10,000 events were counted for each sample.

2.4. Cell proliferation

Mandible and tibia-derived BM-MSCs were seeded on 12-well tissue culture-treated plates (Corning, NY) at 5,000 cells per well and resuspended in growth media. Cultures were then

incubated at 37 ºC and 5% CO_2 and designated for harvest according to pre-determined time points. Cells were then detached using TrypLE™ (Life Technologies, Carlsbad, CA, USA) dissociation reagent every two days for two weeks and enumerated using a hemacytometer to record the final cell number. Triplicate measurements of each time point were used and two measurements were made of each sample to minimize measurement error. Remaining wells were fed with fresh growth media every two days until the time point at which they were designated for enumeration. The population doubling time for each culture was then calculated based on the longitudinal cell counting values up to 13 days by using an online calculator (Roth) (available from http://www.doubling-time.com/compute_more.php) which uses a least squares fitting exponential regression (Eric. W. Weisstein, From MathWorld – A Wolfram Web Resource. http://mathworld.wolfram.com/LeastSquaresFittingExponential.html.)

2.5. Assessment of osteogenic differentiation

Qualitative assessment: Individual 22 x 22 mm glass microscope coverslips were placed at the bottom of each partition of a 6-well plate (Corning Inc., Corning, NY). Tibia and mandible-derived BM-MSCs were then seeded at a density of 100,000 cells per well. Cultures were given 2 mL growth media supplemented with fibroblast growth factor 2 (FGF-2), a growth factor likely to stimulate MSC proliferation and osteogenic differentiation, at 0 ng/mL, 5 ng/mL, or 10 ng/mL. Cells were replaced with fresh corresponding media every three days and kept at 37 ºC and 5% CO_2. On day 10, cells grown on the glass slides were evaluated using the Leukocyte Alkaline Phosphatase Kit (85-L2, Sigma Aldrich®, St Louis, MO). Cells were rinsed with D-PBS and fixed with an acetone buffer consisting of citrate and acetone for thirty seconds. Cells on the glass slide were rinsed twice with tap water and then, in the dark, transferred face-up into staining dishes which contained a light-sensitive staining mixture of distilled water, Napthol, and Fast

Violet B salt (Sigma Aldrich, St Louis, MO). After 30 minutes of staining in the dark, the glass slides were rinsed in a solution of deionized water for 2 minutes and then counterstained in a hematoxylin solution for 10 minutes. Finally the cells on the glass slide were rinsed in a tap water solution for two minutes until the solution was clear.

Quantitative assessment: Similar to the qualitative assessment, tibia and mandible-derived BM-MSCs were seeded on a tissue-culture treated 6-well plate at 100,000 cells per well, and treated with fibroblast growth factor 2 (FGF-2) at 0 ng/mL, 5 ng/mL, or 10 ng/mL. Identical culture conditions were maintained as those in the qualitative assessment. On day 10, cell samples were rinsed, scraped, and then lysed using 300µL of 0.2% Triton®-X-100 solution (Fisher Scientific, Waltham, MA). The collected cells were vortexed, placed on a shaker for 20 minutes, and then frozen. The mixture was later thawed and alkaline phosphatase (ALP) activity was quantified using the QuantiChrome™ Alkaline Phosphatase Kit (BioAssay Systems, Hayward, CA) according to the manufacturer's protocol.

2.6. RNA isolation

RNA extraction was performed on passage 0 cells cultured in growth media from both mandible and tibia-derived BM-MSCs isolated from three pigs. After rinsing twice with D-PBS, the cells were detached from the flask using TrypLE™ (Life Technologies, Carlsbad, CA, USA). After inactivating trypsin with growth media containing FBS, the cells were centrifuged and counted. One million cells were separated from each culture and were again centrifuged directly afterward so that the media could be aspirated. RNA extraction was performed using the RNeasy Mini Kit according to the manufacturer's protocol (Qiagen, Valencia, CA). The concentration of total RNA was then quantified for each sample by Nanodrop ND-1000 (Thermo Scientific,

Wilmington, DE) according to the manufacturer protocol. RNA quality was also evaluated by assessing the 260/280 and 260/230 ratios on the same machine.

2.7. Microarray assay

A total of 3 pairs of RNA samples extracted from passage 0 tibia and mandible BM-MSC cultures of three pigs were used for this assay. Ten micrograms of RNA per sample was submitted to The Ohio State University Genomics (Microarray) Shared Resource department. The quality of total RNA was confirmed using an Agilent 2100 Bioanalyzer (Agilent Technologies, Palo Alto, CA) to ensure an RNA integrity number (RIN) above 9. Subsequently, double-stranded cDNA was generated from total RNA, labeled and fragmented with the GeneChip WT Plus reagent kit (Affymetrix, Santa Clara, CA), then hybridized to the Affymetrix GeneChip® Porcine Genome Array (Santa Clara, CA) which contains 23,937 probe sets to evaluate 20,201 genes. The array was scanned with the GeneChip Scanner 3000, normalized using the RMA algorithm in the Expression Console, and analyzed with the Transcriptome Analysis Console 2.0 (TAC 2.0) (Affymetrix).

Analyzed data collected from TAC 2.0 was sorted for Tukey's bi-weight average signals (log2) to obtain the highly abundant transcriptomes, which have a cut-off point of 10.57, 75% of the highest gene expression of 14.09. Same set of data was then sorted to obtain the differentially expressed genes, which was characterized by the ANOVA p-value < 0.05. Fold-change of 1.5 was chosen as the cut-off point since it is the point where the two cells were separated into 2 individual hierarchical clusters (Fig. 8). The gene symbols were converted to Entrez Gene ID using the Gene Accession Conversion Tool from Database for Annotation, Visualization, and Integrated Discovery (DAVID) v. 6.7. During this process, the corresponding Entrez Gene ID was chosen based on the hierarchy of the species. Specifically, ID corresponding to *homo sapiens*

was first chosen, and when *homo sapiens* was absent, s*us scrofa* was prioritized, followed by *mus musculus*. Subsequently, any duplicates and uncharacterized proteins were eliminated, while the unrecognized genes with names ended with "-like" were matched to their human homologs in Uniprot.org. Functional annotation was performed on the highly abundant transcriptomes and differentially expressed genes using the clustering tool in DAVID. Finally, the microarray data will be deposited in the NCBI Gene Expression Omnibus prior to manuscript publication.

2.8. Reverse-transcription Real-time polymerase chain reaction (RT-PCR):

Isolated RNA samples (3 pairs) as mentioned above were used for this test. Briefly, for each RNA sample, 1 µg of total RNA was reverse transcribed to cDNA using the SuperScript III First-Strand Synthesis System for RT-PCR kit according to the manufacturer's protocol (Invitrogen, Life Technologies, Grand Island, NY). The samples were kept on ice throughout the procedure, except during pipetting and during MasterCyler (Eppendorf®, Foster City, USA) application. Resultant cDNA was diluted 1:1 using 30 µl of sterile water and stored at -20 ºC until all samples were prepared for real-time PCR assay.

Real-time PCR assay was conducted to assess the mRNA expression of two neural crest-associated genes, *BMP-4* and *Nestin*. Forward/reverse primer sets were designed using Primer-BLAST (NCBI, Bethesda, MD) for *Nestin* (fragment size 94 base pair (bp); forward, 5'-TCTCTCAGCATCTTGGACCCTA -3'; reverse, 3'- TAGGACTCAGGACAGAGAGCAA -5') and housekeeping gene *β–actin* (fragment size 179 bp; forward, 5'-TCCCTGGAGAAGAGCTACGA-3', reverse, 5'- TAGAGGTCCTTGCGGATGTC-3'). The primer set for porcine neural crest-related protein *BMP-4* was commercially available from Qiagen (RT² qPCR Primer Assay for Pig BMP4, Product 330001, Qiagen, Valencia, CA). These primer sets were tested for efficacy along with a primer set for known house-keeping gene *β*-

actin. The scouting trial demonstrated that the BMP-4 primer set and one of the *Nestin* primer sets were sufficiently efficacious to detect levels of the associated gene transcripts (see Table 1). These primers were subsequently used for the PCR assay. In order to detect the expression of *BMP-4* and *Nestin*, real-time PCR was performed using iQ-SYBR Green Supermix (Bio-Rad, Hercules, CA) and the iCycler (Bio-Rad, Hercules, CA) according to the manufacturer's protocols. Duplicate trials were completed for each cDNA sample.

For each of the genes investigated, the expression was calculated using the comparative C_T method (or $2^{-\Delta\Delta Ct}$ method). Briefly, the CT values of PCR sample duplicates were averaged and normalized to *β-actin*, which derived ΔCt. The average ΔCt value obtained from the PCR reaction of each mandible-derived sample was further normalized to the average ΔCt value obtained from the tibia-derived sample corresponding to the same animal. Gene expression comparison was then calculated between sites (mandible vs tibia) in terms of the fold of change.

Statistical analysis:

One-way ANOVA tests were used to compare tibial and mandibular BM-MSC microarray data as well as the alkaline phosphatase assay results. Pearson's tests were used to calculate the coefficient of correlation in the microarray data. For proliferation data, cell doubling times were compared using the Mann-Whitney U test. For normally distributed data, paired student t-tests were used. A p-value of <0.05 was considered significant for all analyses. All statistical analyses were performed using SPSS v. 20 software (IBM, Chicago, IL).

3. RESULTS

Bone marrow aspiration and BM-MSC culturing:

Bone marrow aspirations were successful from all four pigs used in the study. Recovered volumes ranged from 15-30 mL from the tibial sites and 10-18 mL from mandibular sites. BM-MSC isolation and expansion were achieved from each aspiration uneventfully. BM-MSCs isolated from mandibular bone marrow aspirates were visibly less abundant during the early days of culturing when compared to parallel BM-MSC cultures from tibial aspirates. Morphologically, mandibular BM-MSCs demonstrated a more prominent spindle-shaped cell body than tibial BM-MSCs with several stretched-out cell processes whereas tibial BM-MSCs were more epithelioid in in appearance (Fig. 2).

Verification of MSC identity:

Flow cytometry confirmed that the cells isolated from both locations exhibited positive expression for all MSC surface markers investigated: CD105, CD44, and CD90. Conversely, they were negative for expression of hematopoietic markers CD11b and CD45.

Proliferation of tibial and mandibular BM-MSCs:

BM-MSCs isolated from both sites demonstrated solid proliferation during early passages of subculture. Generally, noticeable slowdown in proliferation was not observed until approximately passage 5 for tibial BM-MSCs and passage 7 for mandibular BM-MSC cultures. In subpopulations seeded for proliferation measurements, considerable variability was noted between subjects for both mandible and tibia-derived BM-MSCs. Some subcultures reached over-confluence by two weeks after initial seeding, which resulted in a decrease instead of increase of

total cell number. Nevertheless, by calculating cell doubling times of subcultures without post-confluence, we found that the overall (all samples averaged) proliferation rate of mandible-derived BM-MSCs was significantly faster than that of tibial BM-MSCs (Fig. 5). The average cell doubling time calculated based on serial cell number counts during the 13 days of subculture was significantly lower for mandibular BM-MSCs than tibial BM-MSCs (Mann-Whitney U test, $p<0.01$)

Osteogenic differentiation of tibial and mandibular BM-MSCs with and without FGF-2:

Even with only standard growth media used for culture of all BM-MSCs, the cultured cells demonstrated a certain degree of osteogenic differentiation as reflected by positive alkaline phosphatase (ALP) activity. Analysis of trials with and without FGF-2 addition confirmed that mandibular BM-MSC ALP activities were 3.3-fold (factorial ANOVA, $p<0.001$) to those of tibial origin (Fig. 10). For all trials, and at all time points, ALP activity was higher for mandibular BM-MSCs than tibial BM-MSCs (Fig. 11), regardless of presence or absence of FGF-2 (5 ng/mL and 10 ng/mL). Moreover, the addition of FGF-2 did not significantly increase ALP activity relative to the control groups in which only growth media was used (Fig. 11). Staining for ALP showed that positive staining was stronger at day 10 than day 5, with positive BM-MSCs forming clusters. At the periphery where less BM-MSCs were present, ALP-positive clusters were less abundant. At day 10, the contrast between ALP produced by mandibular and tibial BM-MSCs also became more apparent than that at day 5 (Fig. 12).

Comparison of gene (mRNA) expression through microarray assay:

The overall coefficient of correlation between gene expression of BM-MSCs isolated from both locations was significant (Pearson's test = 0.99, $p<0.001$). For differentially expressed

genes, the correlation reduced as the cut-off point of the fold-change increased. The correlation was 0.98 ($p < 0.001$), 0.84 ($p < 0.001$), and 0.48 ($p = 0.82$) for cut-off points of 1, 1.5, and 2.0, respectively. For fold-change above 2.0, when the data was separated into upregulated and downregulated genes, the Pearson correlation was 0.98 and 0.85, which was significant ($p < 0.001$). The correlations were illustrated as scatter plots (Fig. 7).

Based on a 10.57 cut-off of the bi-weight average log2 signals, there were 364 and 370 of highly abundant transcriptomes expressed in mandibular and tibial BM-MSCs, respectively, and only 5.59% (41 genes) were mismatched. Using DAVID's functional annotation clustering tool, it was found that both mandibular and tibial BM-MSCs were enriched in developmental processes such as angiogenesis, ossification, and muscle development, as well as some essential cytoskeletal functions such as cell motion, anti-apoptosis and extracellular matrix organization. The enrichment scores corresponding to the biological processes are listed in Table 1. All of the mentioned functions were significantly enriched (EASE score ≤ 0.05), while a few functions did not meet significance after Benjamini–Hochberg false discovery rate (FDR) corrections.

Above 2.0 fold change, only 14 genes were differentially expressed in mandibular BM-MSCs vs. tibial BM-MSCs, with 8 down-regulated and 6 up-regulated genes. DAVID could not annotate these genes into functional clusters. Using a criterion of 1.5 fold of difference, a total of 47 genes were found to be differentially expressed at the mRNA level between mandibular and tibial BM-MSCs, which consisted of 24 down-regulated and 23 up-regulated genes. DAVID functional annotation on this set of differential expressed genes showed that mandibular BM-MSCs were enriched in sensory perception and neurological system process, as well as protein dimerization activity, while tibial BM-MSCs were enriched in cell component lysosome (Table 2). Similar to the clustering of the highly abundant transcriptomes, the significance in enrichment did not persist after Benjamini–Hochberg FDR correction. The complete lists of the down-regulated and up-regulated genes are presented in Table 3 and Table 4, respectively.

The expression profiles of BM-MSCs isolated from different locations only categorized in separated clusters at 1.5 fold of difference, but not at 2.0 fold of difference, as presented in the hierarchical clustering heat map (Fig. 8). While the functions of most of these genes were unknown or not strongly relevant to osteogenesis or angiogenesis based on current understandings, two particular genes, *nestin* and *BMP-4* are both cranial neural crest-related genes and demonstrated higher expression in mandibular BM-MSCs than tibial BM-MSCs (1.23-fold and 1.79-fold, respectively, ANOVA, $p<0.05$).

RT-PCR:

Expression of neural crest-associated mRNA for *BMP-4* and *nestin* showed the same trend of differences between BM-MSCs from the two sites. Specifically, they were both expressed more strongly in mandibular BM-MSCs than tibial BM-MSCs, but statistically the differences were not significant (Fig. 9).

4. DISCUSSION

The purpose of this study was to compare BM-MSCs from the mandible to those from the tibia in a pig model. Specifically, we investigated their gene expression and some properties related to skeletal tissue regeneration including expression of mesenchymal stem cell markers, proliferation and osteogenic differentiation.

While bone marrow aspiration from pig tibiae or iliac crests has been routinely and consistently performed by many researchers, we established a method to aspirate bone marrow from the pig mandible for the first time. Based on experience from the four pigs used in this

study, 10-18 mL bone marrow can be aspirated from the mandibular symphyseal region in four month old pigs through a single needle insertion. Although the abundance of bone marrow in the mandibular symphyseal region appears to be smaller than that from the tibia, 10-18 mL of bone marrow was adequate for subsequent isolation and expansion of BM-MSCs. Various studies have described isolating MSCs from a number of craniofacial sources including dental pulp and the periodontal ligament but few studies exist which describe harvesting stromal cells from craniofacial bone marrow. Due to the small size of craniofacial bones relative to long bones, the marrow volume is believed to be less abundant. Accordingly, previous investigators who attempted to isolate BM-MSCs from craniofacial bones have done so by rinsing trabecular bone fragments recovered at human third molar extractions sites[39] or by flushing bone marrow from the superior alveolar ridge through extraction sockets[45, 86] in rats. Therefore, we are the first group that directly aspirated appreciable volumes (11-18 mL) of bone marrow directly from the symphyseal area of juvenile porcine mandibles.

Through flow cytometry analysis, we confirmed that the stromal cells isolated from mandibular bone marrow are indeed mesenchymal stem cells (MSC). More specifically, both mandible and tibia BM-MSCs strongly expressed CD105/endoglin, CD90, and CD44 (surface markers of MSCs) and lacked expression of CD11b and CD45, surface markers expressed by hematopoetic stem cells. These data corroborate findings from other investigators who isolated BM-MSCs from pig and human iliac crest and long bones and found them to be positive for CD105, CD44, and CD90[88-90], while negative for CD11b[91] and CD45[88, 90-92].

The ability of fast replication is an important property of MSCs needed for tissue engineering. Through a series of cell culturing and passaging experiments, we found that mandibular BM-MSCs proliferated significantly faster than tibial BM-MSCs. The mandibular BM-MSCs also outlasted the tibial BM-MSCs in maintaining a high proliferation rate through later passages. Our findings about BM-MSC proliferation are consistent with those reported by

other groups[39, 45, 86], who phenotypically compared craniofacial and lower extremities BM-MSCs from humans or rats. Specifically, Akintoye's group evaluated the proliferative capacity of human BM-MSCs isolated from the mandible, maxilla, and iliac crest cells over the same time period (14 days) and showed that both maxillary and mandibular BM-MSCs proliferated faster than iliac crest BM-MSCs. They also reported delayed senescence of orofacial-derived BM-MSCs compared to iliac crest BM-MSCs. Similarly, rat mandibular BM-MSCs exhibited stronger proliferation and anti-apoptotic potentials as compared to long bone BM-MSCs[45, 86]. Morphologically, the iliac crest is a flat bone, while the tibia is a long bone. Anatomically, however, both the iliac crest and the tibia are bones of the lower extremity, and embryonically they share the same mesoderm origin. On the other hand, the jaws are craniofacial bones with both the mesoderm and cranial neural crest cells contributing to their embryonic development[87]. More importantly, cells expressing neural crest markers are known to be more pluripotent, a feature believed to contribute to the survival of MSCs in hypoxia after transplantation[93, 94]. Therefore, despite the difference in research subjects between the present study and the Akintoye et al.'s and Dong et al.'s studies[39, 86], the combined data suggest that the cranial neural crest-derived BM-MSCs have a stronger proliferation potential than those from their mesodermal-derived counterparts in the limbs.

The ability of osteogenic differentiation is another important property of BM-MSCs for skeletal tissue engineering. In the present study, osteogenic capacity was compared by assessing ALP activity, an indicator for early osteogenic differentiation. Previous studies including those from our lab have evaluated osteogenic capacity of BM-MSCs in varied ways[38, 45, 95, 96]. Typically, the cultured cells were induced by supplementing the culturing media with ascorbic acid, dexamethasone, and β-glycerophosphate or using other commercially developed kits. As we previously found, however, even without osteogenic induction, the cultured BM-MSCs demonstrated a certain degree of ALP activity[38], suggesting that some of the replicated cells may

be committed to the osteogenic lineage during *in vitro* expansion. This was confirmed in the current study, and the mandibular BM-MSCs appear to be stronger ALP producers than tibia BM-MSCs. We also found that these site-related differences were not changed by the addition of FGF-2. Previously we showed that when FGF-2 was used together with osteogenic media, osteogenic differentiation measured by ALP activity and Runx-2 expression was enhanced[38]. Other investigators have also shown that FGF-2 at concentrations as low as 1 ng/mL can increase ALP activity in human MSCs placed in osteogenic media[97]. The present data, however, seem to suggest that FGF-2 by itself does not act as an osteogenic inducer for either mandibular or tibial BM-MSCs. This may indicate that osteogenic inducers are required for FGF-2 to augment ALP activity in these cells and additional studies are warranted to evaluate this speculation. In a related study on rats, Aghaloo et al. and Dong et al. observed significantly greater ALP activity and osteocalcin expression in mandibular BM-MSCs than long bone BM-MSCs[45, 86]. The same trend of enhanced osteogenic potential of craniofacial-derived BM-MSCs was also reported in humans using small marrow samples from third molar extraction sites[39]. Although we tested ALP activity without the addition of common osteogenic inducers while the other two groups did use osteogenic media, our findings are consistent with theirs. Combined, these data suggest that craniofacial BM-MSCs are likely advantageous to long bone BM-MSCs in terms of the ability of osteogenic differentiation. It is worth noting that our present data only reveal a small part of the osteogenic capacity of BM-MSCs as we only studied ALP activity. Future studies are needed to examine the expression of markers indicative of middle and late stage osteogenic differentiation such as osteopontin and osteocalcin, respectively[68, 98, 99], as well as type I collage and mineral production.

To assess whether this difference in proliferation and osteogenic differentiation is relevant to variation in gene expression, especially neural crest-related genes, we conducted a microarray assay. The results found that a total of 383 genes were significantly different between

mandibular and tibial BM-MSCs (ANOVA test, $p < 0.05$), out of which 47 genes demonstrated >1.5 fold of differences, between the two locations. Generally gene expression with >2 fold of difference is considered as differentially expressed. Based on the 14 differentially expressed genes identified by the 2-fold criterion, one would quickly conclude the gene profiles between mandibular and tibial BM-MSCs are very similar. On one hand, as cells from both locations are BM-MSCs, it is not surprising that they have a high similarity in gene expression. On the other hand, however, it does not explain the phenotypical differences between the cells from the two sites, such as proliferation and differentiation as discussed above. Possible explanations become available when the microarray data were analyzed using more sophisticated methods. First, the hierarchical clustering was performed on the set of genes with at least 1.5-fold difference, which revealed a significant incongruence between the primary passages of BM-MSCs isolated from these two locations. Using the same cut-off criterion, DAVID analysis also categorized the gene profile into functional groups, which showed distinct differences between mandibular and tibial BM-MSCs (Table 1). Specifically, mandibular BM-MSCs tended to be enriched in neurological processes and protein dimerization activity. In particular, two of the four genes involved in the protein dimerization activity, *BMP-4* and activating transcription factor (*ATF6*), are both related to cell survival (Teodoro, Ueki) and osteogenesis[100, 101]. *BMP-4* is also specifically a neural-crest gene, and was found critical for stem cell renewal and maintaining pluripotency. *Nestin* was another noteworthy upregulated neural crest marker in mandibular BM-MSCs, but only has a fold change of 1.23. It is also essential for cell proliferation and migration, while maintaining the stemness of the cell[102, 103]. In contrast, tibial BM-MSCs were enriched in cellular component lysosome, which is an organelle involved in the terminal steps of apoptosis[104]. These distinctive clusters , although categorized at a less stringent criterion (1.5 fold instead of 2 fold of difference), at least demonstrate a tendency that mandibular BM-MSCs have a higher chance of survival and osteogenic potential, while tibial BM-MSCs may be more prone to apoptosis, a finding that matches our proliferation and osteogenic differentiation data about these cells.

Next, when the highly abundant transcriptomes expressed were compared between BM-MSCs from the two locations, a distinct difference was also found. More specifically, with 75% of the highest expressed gene which have a log2 of 14.07 being compared, mandibular and tibial BM-MSCs were significantly enriched in angiogenesis and ossification, and other essential cellular functions such as cell motion and extracellular matrix organization (Table 1). Although the particular genes reported to be differentially expressed by Monaco et al. were not the same as ours[70], functional annotation analysis with DAVID found that the categories of genes of long bone BM-MSCs were similar between the two studies. In Monaco's microarray analysis comparing porcine BM-MSCs isolated from long bone and adipose tissue, they found that long bone BM-MSCs have higher angiogenic, osteogenic, migratory, and neurogenic capacity compared to adipose-derived MSCs[70]. In our study, not only did the differentially expressed genes analysis demonstrate a tendency of higher neurogenic capacity in mandibular BM-MSCs than long bone BM-MSCs in the highly abundant transcriptome analysis, mandibular BM-MSCs also demonstrated a tendency for stronger gene expression regulating endochondral ossification and skeletal muscle tissue development. This further explains the difference in osteogenic differentiation and implies that mandibular BM-MSCs are superior in bone regeneration to tibial BM-MSCs.

While microarray analysis is highly efficient in screening thousands of genes, precautions are warranted for the findings and interpretations. The number of subjects used in the present and the Monaco et al. study is relatively low, which may reduce statistical power and increases susceptibility to biases. Thus, additional tests are desired to confirm our gene expression microarray findings. Limited by the scope of this thesis project, however, we were not able to retest a large number of genes using RT-PCR that were found to be statistically differentially expressed between mandible and tibia BM-MSCs. As a result, we only further tested the expression of two genes known to be neural crest related, *BMP-4* and *nestin*, using RT-PCR tests.

The results confirmed the trend reflected by the microarray assay. That is, both *BMP-4* and *nestin* tended to express more strongly in mandibular BM-MSCs than tibial BM-MSCs, although the net differences were less than one fold and did not reach statistical significance. Although *BMP-4* and *nestin* have been used as neural crest markers, their unique function in human development continues to be researched. *BMP-4* is essential for differentiation of mesoderm, including development of craniofacial and appendicular bone, and knockouts of this gene result in embryonic lethality[105]. *Nestin*, an intermediate filament protein, is expressed predominantly in rapidly dividing cells of developing and regenerating tissues and is understood to play an important role in central and peripheral nervous system development[106, 107]. For these reasons, it is understandable why some expression of these proteins is still recorded in tibial BM-MSCs even though are not of neural crest origin.

Although a sample size of four pigs is reasonable for studies of this nature, a greater number of subjects/samples would have increased the statistical power of our results. The number of surgeries required to acquire more samples required greater time and resources than were available. The significant cost of certain aspects of this study, specifically microarray technology, is a related limiting factor. Additionally, the amount of variability between subjects is sufficient to make it challenging reach statistical significance in some instances. As mentioned previously, our assessment of osteogenic capacity is limited in scope because we measured ALP prior to treating with osteogenic media. Greater understanding would be reached by evaluating ALP and other osteogenic markers after treating cells inducers such as dexamethasone, ascorbic acid, and β-glycerophosphate either by additional protein assays or quantitative PCR.

In conclusion, this study establishes that BM-MSCs are readily obtainable from the pig mandible and demonstrates that MSCs from this location express a number of genes differently than those typically recovered from long bone marrow. Our findings not only support the concept of dissimilar embryologic origin between the two types of BM-MSCs, it confirms that

craniofacial-derived BM-MSCs have a distinct advantage in their capacity for bone regeneration due to higher proliferative ability and high propensity toward osteogenic differentiation. Future studies are warranted to evaluate the *in vivo* application of craniofacial-derived BM-MSCs for repair and regeneration of osseous defects.

CONFLICT OF INTEREST

The authors declare no conflict of interest.

ACKNOWLEDGEMENTS

This study was partially supported by the Delta Dental Foundation Master's Thesis Award Program, by support from an AAOF Biomedical Research Award and NIH grant R56DE024172.

CHAPTER 4

RESULTS

Bone Marrow Aspiration and BM-MSC Culturing:

Bone marrow aspirations were successful from all four pigs used in the study. Recovered volumes ranged from 15-30 mL from the tibial sites and 10-18 mL from mandibular sites. BM-MSC isolation and expansion were achieved from each aspiration uneventfully. BM-MSCs isolated from mandibular bone marrow aspirates were visibly less abundant during the early days of culturing when compared to parallel BM-MSC cultures from tibial aspirates. Morphologically, mandibular BM-MSCs demonstrated a more prominent spindle-shaped cell body than tibial BM-MSCs with several stretched-out cell processes whereas tibial BM-MSCs were more epithelioid in in appearance (Fig. 2).

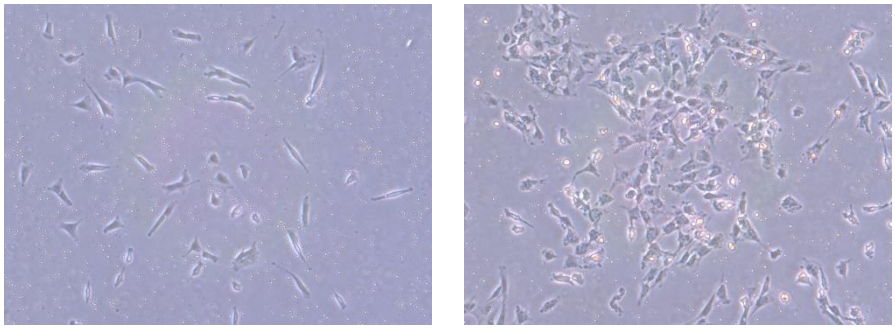

Figure 2. Initial BM-MSC cultures

Verification of MSC identity:

Flow cytometry confirmed that the cells isolated from both locations exhibited positive expression for all MSC surface markers investigated in this study: CD105, CD44, and CD90. Conversely, they were negative for expression of hematopoietic markers CD11b and CD45 (Fig. 3 and 4).

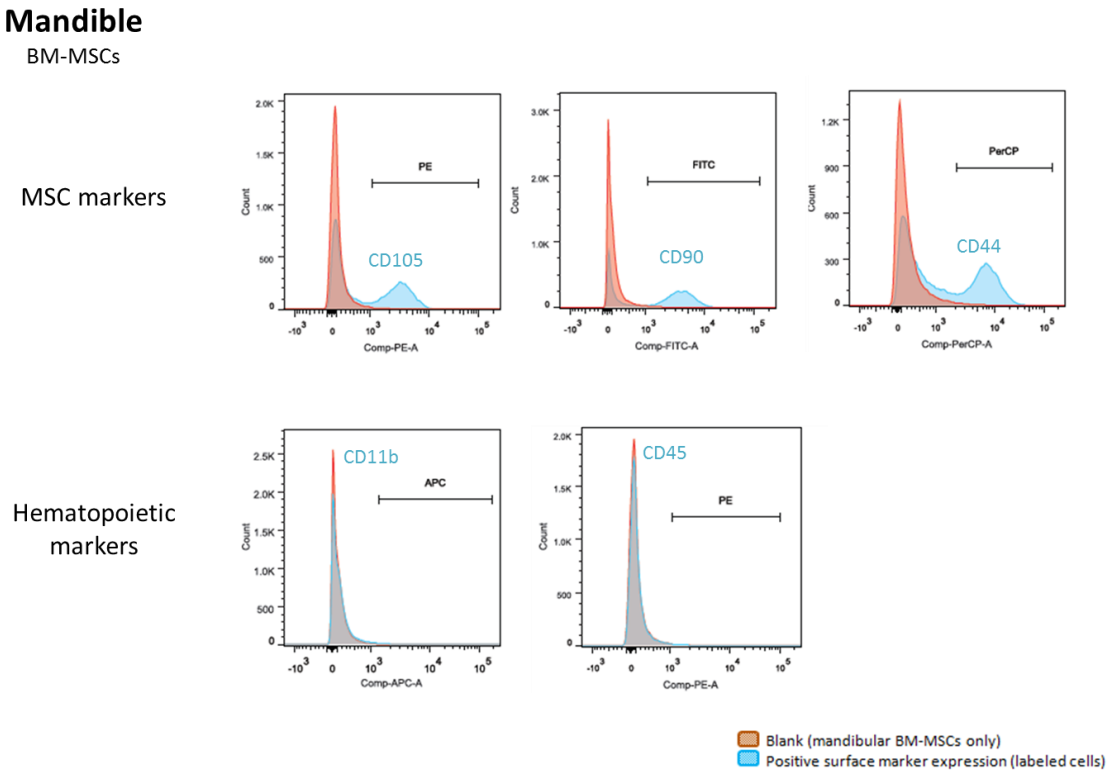

Figure 3. Flow cytometry for mandibular BM-MSCs: CD105, CD44, CD90, CD11b, CD45

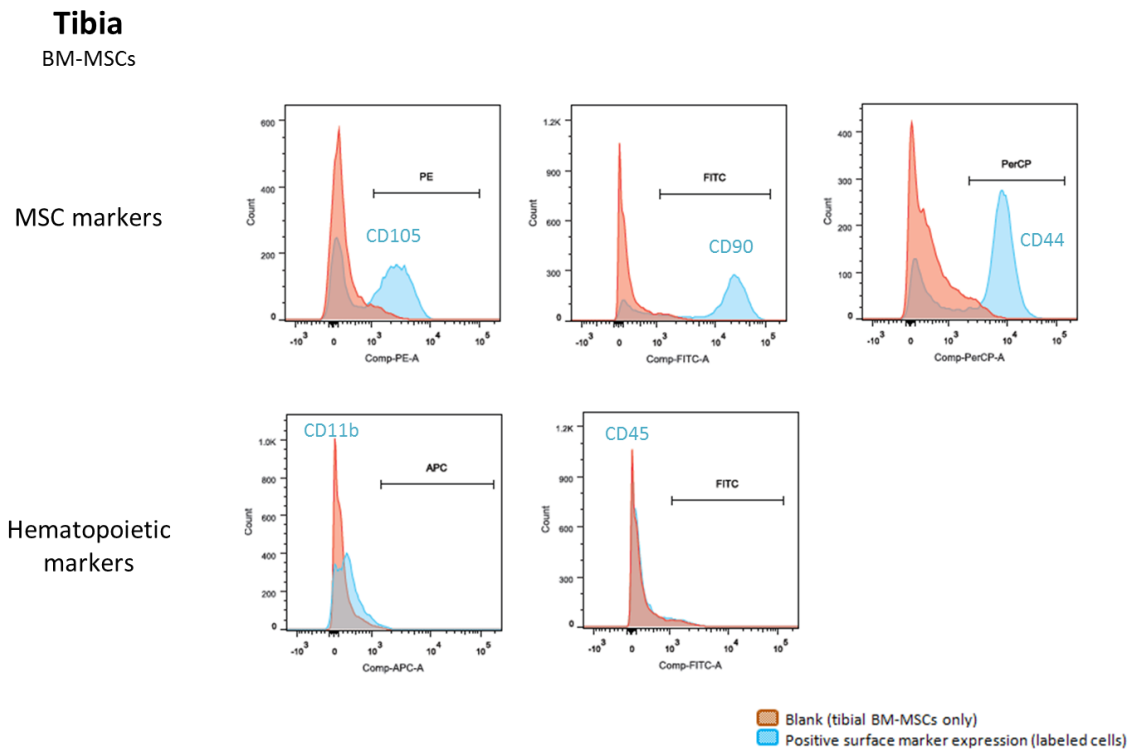

Figure 4. Flow cytometry for tibial BM-MSCs: CD105, CD44, CD90, CD11b, CD45

Proliferation of Tibial and Mandibular BM-MSCs:

BM-MSCs isolated from both sites demonstrated solid proliferation during early passages of subculture. Generally, noticeable slowdown in proliferation was not observed until approximately passage 5 for tibial BM-MSCs and passage 7 for mandibular BM-MSC cultures. In subpopulations seeded for proliferation measurements, considerable variability was noted between subjects for both mandible and tibia-derived BM-MSCs. Some subcultures reached over-confluence by two weeks after initial seeding, which resulted in a decrease instead of increase of total cell number. Nevertheless, by calculating cell doubling times of subcultures without post-confluence, we found that the overall (all samples averaged) proliferation rate of mandible-derived BM-MSCs was

significantly faster than that of tibial BM-MSCs (Fig. 5). The average cell doubling time calculated based on serial cell number counts during the 13 days of subculture was significantly lower for mandibular BM-MSCs than tibial BM-MSCs (Mann-Whitney U test, $p<0.01$)

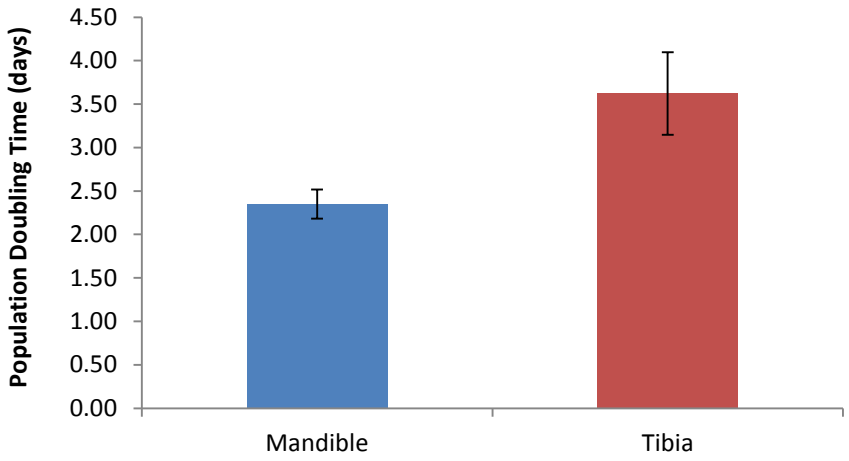

Figure 5. Tibial vs mandibular BM-MSC median population doubling times

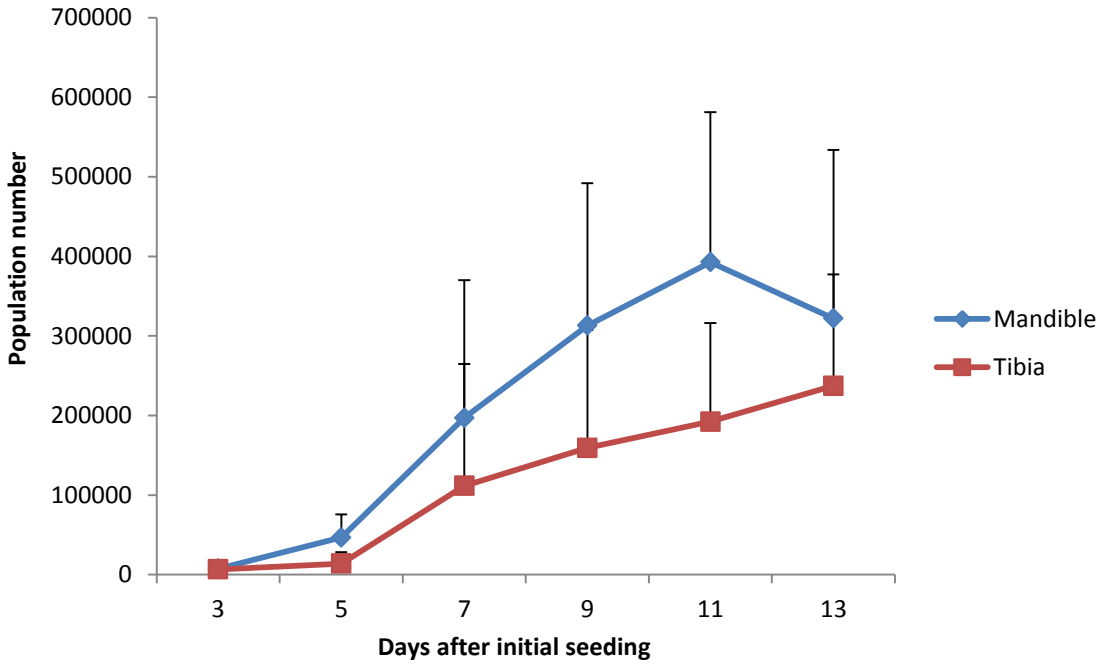

Figure 6. Tibial vs mandibular BM-MSC cell proliferation (seeding performed at Day 0)

Comparison of Gene (mRNA) Expression through Microarray Assay:

The overall coefficient of correlation between gene expression of BM-MSCs isolated from both locations was significant (Pearson's test = 0.99, $p<0.001$). For differentially expressed genes, the correlation reduced as the cut-off point of the fold-change increased. The correlation was 0.98 ($p < 0.001$), 0.84 ($p < 0.001$), and 0.48 ($p = 0.82$) for cut-off points of 1, 1.5, and 2.0, respectively. For fold-change above 2.0, when the data was separated into upregulated and downregulated genes, the Pearson correlation was 0.98 and 0.85, which was significant ($p < 0.001$). The correlations were illustrated as scatter plots (Fig. 7).

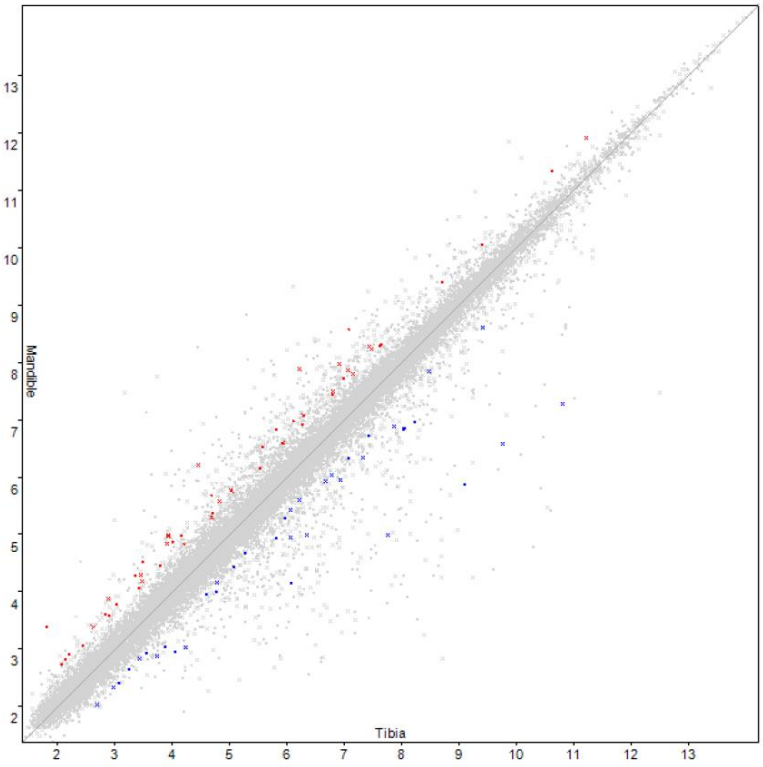

Figure 7: Correlation of the differentially expressed genes between mandibular and tibial BM-MSCs.

Based on a 10.57 cut-off of the bi-weight average log2 signals, there were 364 and 370 of highly abundant transcriptomes expressed in mandibular and tibial BM-MSCs, respectively, and only 5.59% (41 genes) were mismatched. Using DAVID's functional annotation clustering tool, it was found that both mandibular and tibial BM-MSCs were enriched in developmental processes such as angiogenesis, ossification, and muscle development, as well as some essential cytoskeletal functions such as cell motion, anti-apoptosis and extracellular matrix organization. The enrichment scores corresponding to the biological processes were listed in Table 1. All of the mentioned functions were significantly enriched (EASE score ≤ 0.05), while a few functions did not meet significance after Benjamini–Hochberg false discovery rate (FDR) corrections.

Biological Processes	Enrichment Score		EASE score (modified fisher exact p-value)		Benjamini–Hochberg FDR	
	Mand. BM-MSC	Tibial BM-MSC	Mand. BM-MSC	Tibial BM-MSC	Mand. BM-MSC	Tibial BM-MSC
Angiogenesis	6.86	5.68	3.4E-5	1.5E-4	2.6E-3	8.5E-3
Ossification	5.21	4.91	2.6E-6	1.5E-5	3.6E-4	1.2E-3
Endochondral ossification	1.1	-	2.2E-2	-	2.3E-1	-
Skeletal muscle tissue development	1.97	-	4.0E-2	-	3.4E-1	-
Cell motion	3.07	3.98	2.0E-7	1.4E-8	4.0E-5	4.4E-6
Anti-apoptosis	2.59	3.24	7.5E-3	2.4E-3	1.1E-1	5.5E-2
Extracellular matrix organization	3.32	9.33	1.6E-9	1.4E-12	1.1E-6	1.3E-9
Cytoskeleton organization	4.24	7.15	5.1E-6	4.8E-6	5.7E-4	5.3E-4

Table 1: Functions significantly enriched in highly abundant transcriptomes between mandibular and tibial BM-MSCs.

Above 2.0 fold change, only 14 genes were differentially expressed in mandibular BM-MSCs vs. tibial BM-MSCs, with 8 down-regulated and 6 up-regulated genes. DAVID could not annotate these genes into functional clusters. Using a criterion of 1.5 fold of difference, a total of 47 genes were found to be differentially expressed at the mRNA level between mandibular and tibial BM-MSCs, which consisted of 24 down-regulated and 23 up-regulated genes. DAVID functional annotation on this set of differential expressed genes showed that mandibular BM-MSCs were enriched in sensory perception and neurological system process, as well as protein dimerization activity, while tibial BM-MSCs were enriched in cell component lysosome (Table 2). Similar to the clustering of the highly abundant transcriptomes, the significance in enrichment did not persist after Benjamini–Hochberg FDR correction. The complete lists of the down-regulated and up-regulated genes are presented in Table 3 and Table 4, respectively.

Location	Gene ontology (GO) terms	Category	EASE score (modified fisher exact p-value)	Benjamini–Hochberg FDR
Mandibular	Biological process	Sensory perception of chemical stimulus	1.7E-2	1.0E0
		Neurological system process	4.9E-2	1.0E0
	Molecular function	Protein dimerization activity	1.5E-2	7.0E-1
Tibia	Cellular component	Lysosome	3.5E-2	2.4E-1

Table 2: Functions significantly enriched in differentially expressed genes above 1.5 fold change between mandibular and tibial BM-MSCs.

Gene Symbol	Description	Fold Change
F13A1	coagulation factor XIII, A1 polypeptide	-9.36
LOC100517092	carboxypeptidase M-like	-9.07
HPSE	heparanase	-6.87
LAMA2	laminin, alpha 2	-2.57
LOC100521735	N-acylethanolamine-hydrolyzing acid amidase-like	-2.4
LOC100523534	olfactory receptor 4B1-like	-2.31
RGS2	regulator of G-protein signaling 2, 24kDa	-2.3
DEPTOR	DEP domain containing MTOR-interacting protein	-2.15
NAGA	N-acetylgalactosaminidase, alpha-	-1.99
C18H7orf58	chromosome 7 open reading frame 58	-1.98
IL10RA	interleukin 10 receptor, alpha	-1.98
LOC100737106	olfactory receptor 8S1-like	-1.79
SUCLA2	succinate-CoA ligase, ADP-forming, beta subunit	-1.76
DOCK10	Dedicator of cytokinesis protein 10	-1.72
LOC100513900	immunoglobulin superfamily DCC subclass member 4-like	-1.67
BAI2	brain-specific angiogenesis inhibitor 2	-1.62
LOC100153656	kelch/ankyrin repeat containing cyclin A1 interacting protein	-1.58
C1QTNF7	C1q and tumor necrosis factor related protein 7	-1.58
LOC100154725	olfactory receptor 4K3-like	-1.57
PECAM1	platelet/endothelial cell adhesion molecule 1	-1.54
GRPR	gastrin-releasing peptide receptor	-1.53
CYP4A11	cytochrome P450 4A11-like	-1.52
KCNT2	potassium channel, subfamily T, member 2	-1.51
LOC100511910	coronin-2A-like	-1.5

Table 3: Differentially expressed genes above 1.5-fold of downregulation in mandibular BM-MSCs.

Gene Symbol	Description	Fold Change
REM1	RAS (RAD and GEM)-like GTP-binding 1	1.5
LOC100517545	olfactory receptor 52B4-like	1.54
LOC100152428	multidrug resistance-associated protein 1-like	1.56
PLXNA2	plexin A2	1.57
DSCAML1	Down syndrome cell adhesion molecule like 1	1.58
LOC100516444	uncharacterized LOC100516444	1.58
SYT1	synaptotagmin I	1.58
LOC100737436	protein S100-A16-like	1.58
PGCP	plasma glutamate carboxypeptidase	1.59
LOC100516627	olfactory receptor 4F3/4F16/4F29-like	1.6
ATF6	activating transcription factor 6	1.6
LOC100523238	olfactory receptor 2AE1-like	1.63
KIF21A	kinesin family member 21A	1.67
RTKN2	rhotekin-2-like	1.7
DENND2C	DENN/MADD domain containing 2C	1.77
BMP4	bone morphogenetic protein 4	1.79
NR5A2	nuclear receptor subfamily 5, group A, member 2	1.98
LOC100157532	copine-4-like	2.03
MIR27B	microRNA mir-27b	2.04
LOC100512015	leucine-rich repeat LGI family member 3-like	2.08
AKR1CL1	aldo-keto reductase family 1, member C-like 1	2.79
ANO1	anoctamin 1, calcium activated chloride channel	3.16
TRPA1	transient receptor potential cation channel, subfamily A, member 1	3.36

Table 4: Differentially expressed genes above 1.5-fold of upregulation in mandibular BM-MSCs.

The expression profiles of BM-MSCs isolated from different locations only categorized in separated clusters at 1.5 fold of difference, but not at 2.0 fold of difference, as presented in the hierarchical clustering heat map (Fig. 8).

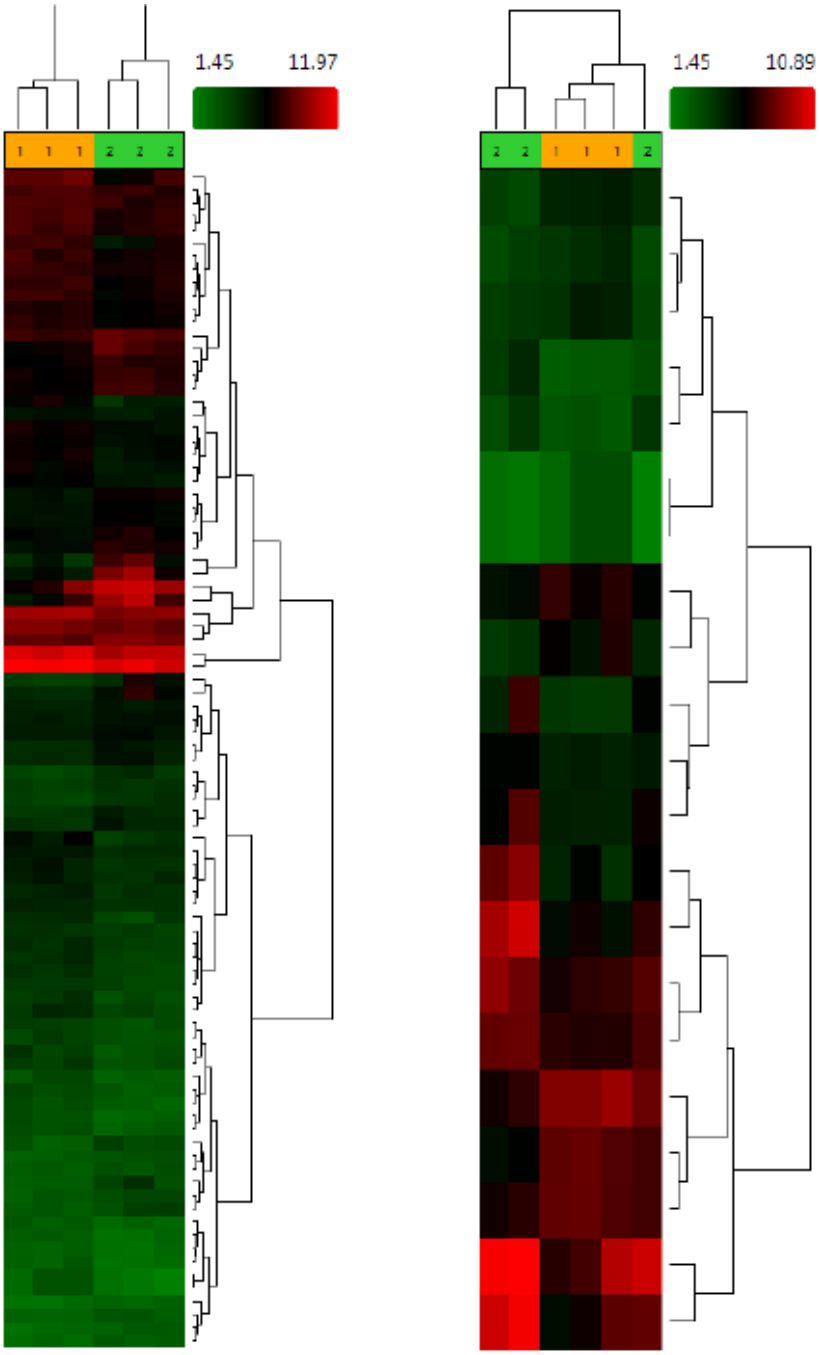

Figure 8: Heat map showing hierarchical clustering of differentially expressed genes above 1.5 fold change (left) and above 2.0 fold change (right). Group 1 (yellow) represents mandibular BM-MSCs, while Group 2 (green) represents tibial BM-MSCs.

While the functions of most of these genes were unknown or not strongly relevant to osteogenesis or angiogenesis based on current understandings, two particular genes, *nestin* and *BMP-4* are both cranial neural crest-related genes and demonstrated higher expression in mandibular BM-MSCs than tibial BM-MSCs (1.23-fold and 1.79-fold, respectively, ANOVA, $p<0.05$).

RT-PCR:

Expression of neural crest-associated mRNA for *BMP-4* and *nestin* showed the same trend of differences between BM-MSCs from the two sites. Specifically, they were both expressed more strongly in mandibular BM-MSCs than tibial BM-MSCs, but statistically the differences were not significant (Fig. 9).

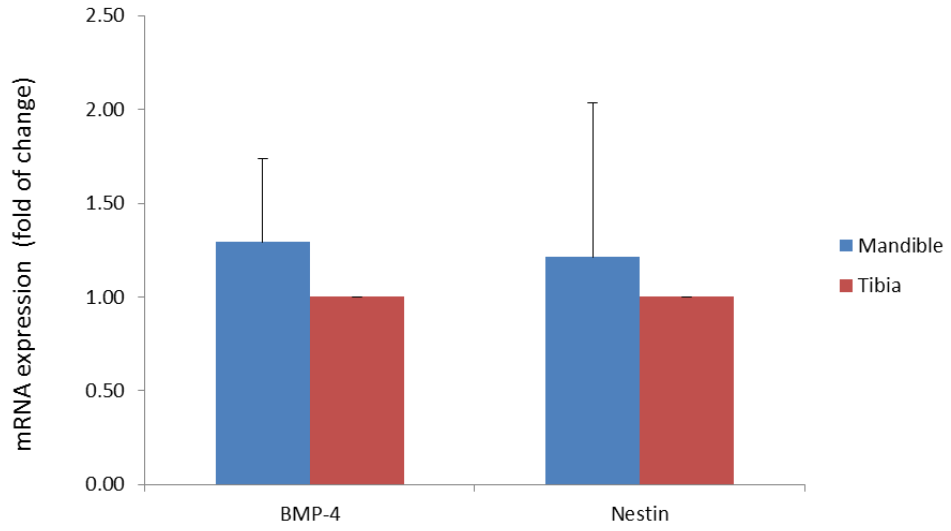

Figure 9. Fold change mRNA expression of BMP-4 and Nestin in mandible vs tibia BM-MSCs

Osteogenic differentiation of tibial and mandibular BM-MSCs with and without FGF-2:

Even with only standard growth media used for culture of all BM-MSCs, the cultured cells demonstrated a certain degree of osteogenic differentiation as reflected by positive alkaline phosphatase (ALP) activity. Analysis of trials with and without FGF-2 addition confirmed that mandibular BM-MSC ALP activities were 3.3-fold (factorial ANOVA, $p<0.001$) to those of tibial origin (Fig. 10). For all trials, and at all time points, ALP activity was higher for mandibular BM-MSCs than tibial BM-MSCs (Fig. 11), regardless of presence or absence of FGF-2 (5 ng/mL and 10 ng/mL). Moreover, the addition of FGF-2 did not significantly increase ALP activity relative to the control groups in which only growth media was used (Fig. 11). Staining for ALP showed that positive staining was stronger at day 10 than day 5, with positive BM-MSCs forming clusters. At the periphery where less BM-MSCs were present, ALP-positive clusters were less abundant. At day 10, the contrast between ALP produced by mandibular and tibial BM-MSCs also became more apparent than that at day 5 (Fig. 12).

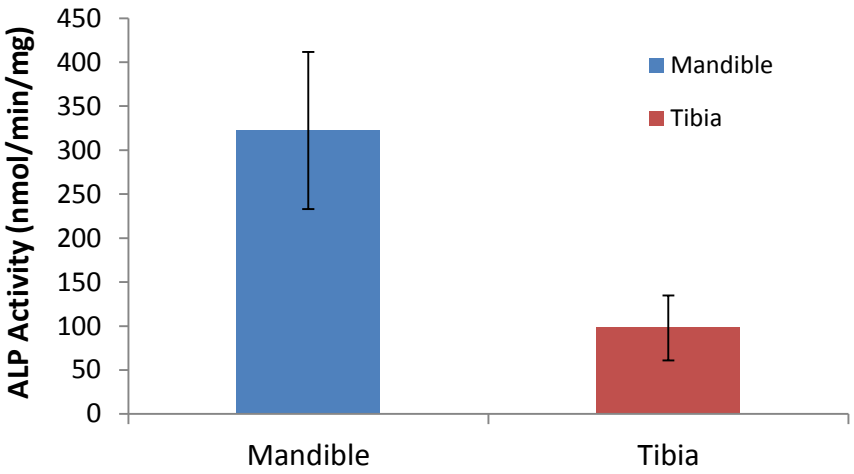

Figure 10. ALP production: pooled results of mandible and tibia BM-MSCs with and without addition of FGF-2

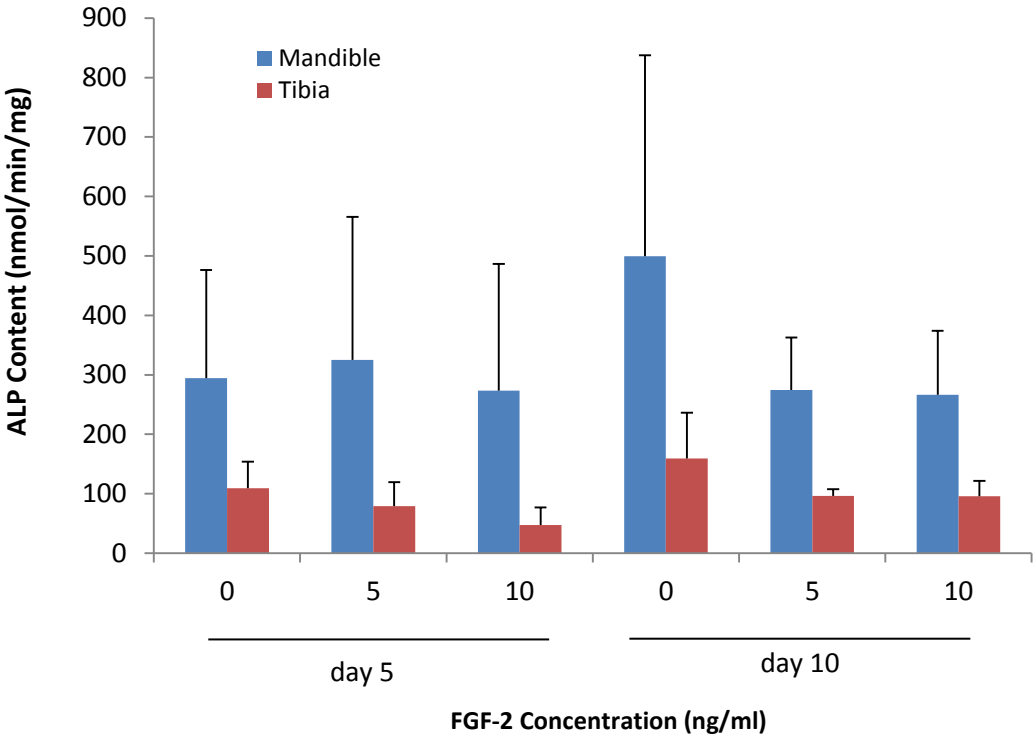

Figure 11. ALP production of mandible and tibia BM-MSCs with and without addition of FGF-2 at day 5 and day 10

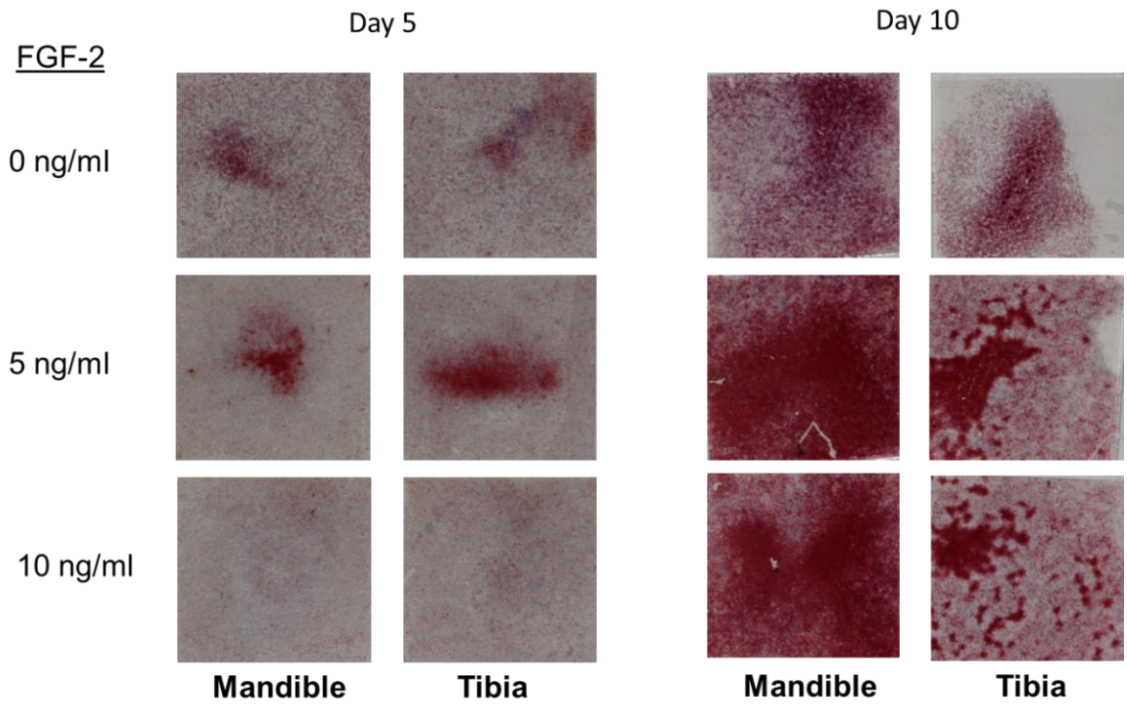

Figure 12. ALP staining of mandible and tibia BM-MSCs in growth media with and without addition of FGF-2 at day 5 and day 10.

Triple-layer Cell Sheet Formation

BM-MSCs from both the tibia and mandible were able to form triple-layer cell sheets, but did show differences between them. After forty-eight hours of incubation, mandibular BM-MSC cell sheets were formed on 12-well thermo-responsive plates (Nunc™ UpCell™, Thermo Scientific) at an initial seeding density of 200,000 cells per well ~(57K/cm^2, Fig. 13). Tibia BM-MSCs seeded at this density did not form intact cell sheets with the same incubation period. Instead, viable tibia cell sheet formation required an initial seeding density of 400,000 cells per well on 12-well plates (~114K/cm^2) or 200,000 cells per well on 24-well plates. Regardless of the initial seeding density, successfully formed cell sheets were adherent to CellSTART™-coated culture dishes

after 30 minutes and the addition of subsequent layers was successful and repeatable (Fig. 13). On the other hand, when the above described low seeding densities were used, the cell sheets tended not to release from the polymer surface of the dish with intact sheet structure maintained, voiding further manipulation of adding more layers. Thus, low-density sheets tended to be easily friable and had a mosaic pattern with tattered edges, discontinuity, and voids. In contrast, high density sheets had minimal voids and were reliably transferrable to other surfaces using gentle pipetting techniques.

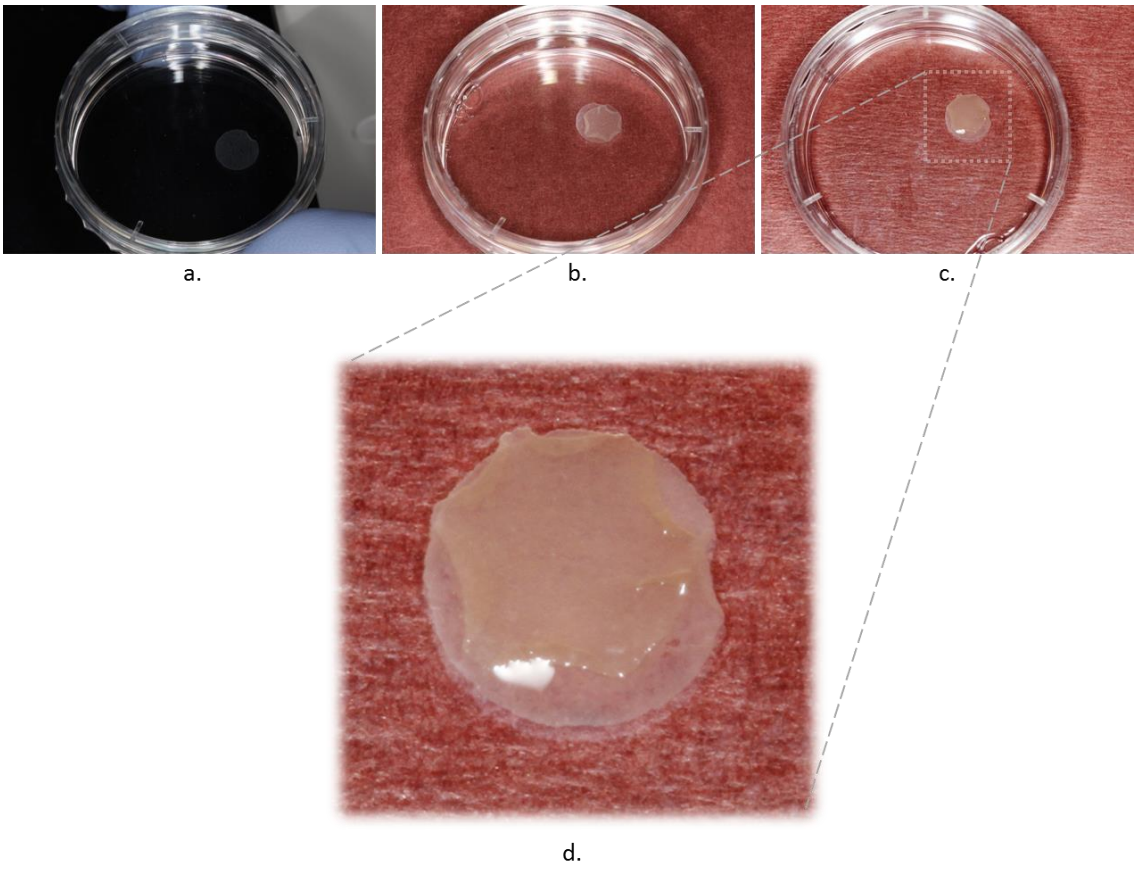

Figure 13. Gross specimen: mandibular BM-MSC cell sheets in single (a), double (b), and triple (c) layer formation with magnified view of the triple layer addition (d).

Viability and Histologic Assessment of Porcine BM-MSC Sheets:

Twenty four hours after incubation, triple-layer cell sheets fabricated from tibia and mandible-derived BM-MSCs remained intact. Using simple means such as micropipette tip or a small laboratory spatula, they could be peeled off of the surface of the culture dish as an intact sheet and then transferred to a microscope slide. Subsequent fluorescent live/dead staining demonstrated that mandibular BM-MSCs layered sheets had fewer dead cells than tibial BM-MSCs (3.13% vs. 10.25%, t-test, $p<0.05$) during the same incubation period (Fig. 14).

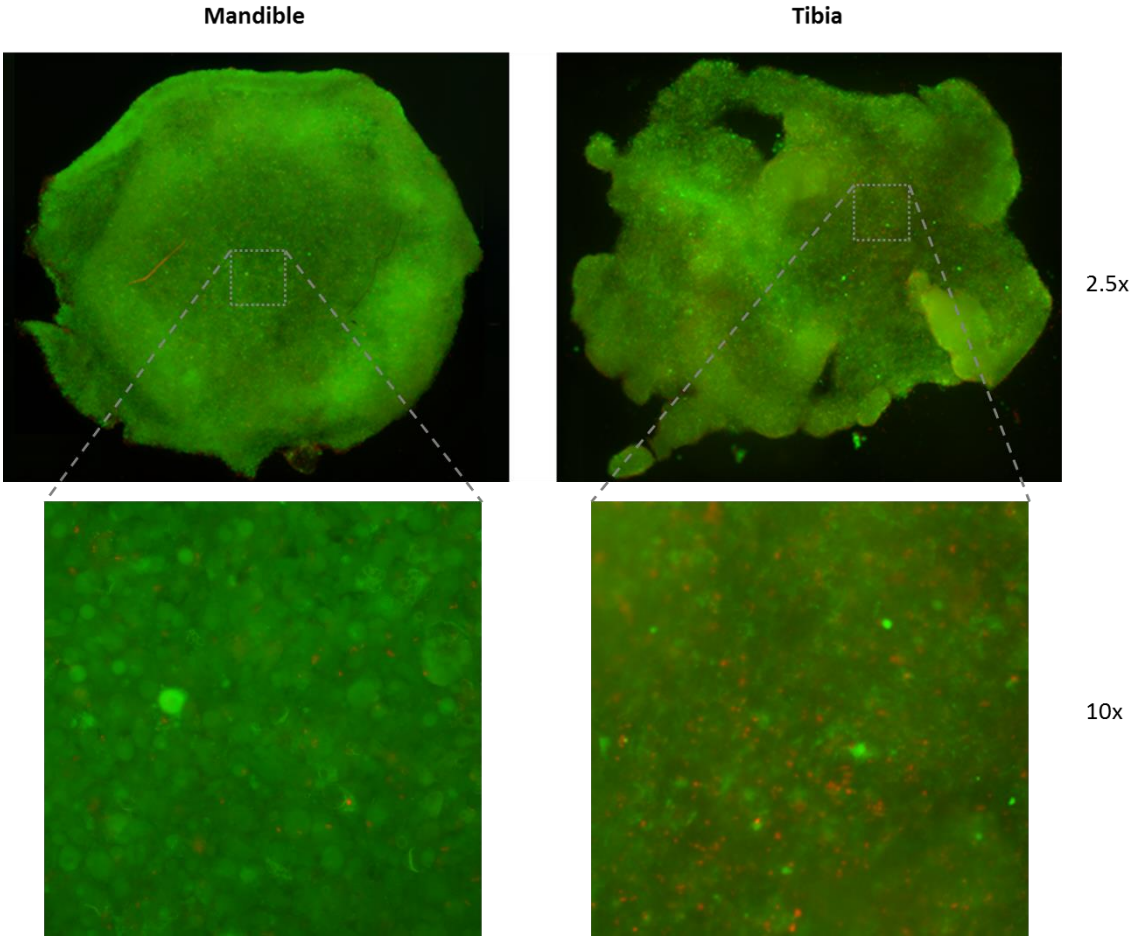

Fig 14. Fluorescent Live/Dead staining for mandibular and tibial BM-MSC triple layer cell sheets [fluorescence: green (live), red (dead)]

H & E staining was performed on cell sheets previously used for the live/dead assay as well as on cell sheets not exposed to live/dead assay. Under a light microscope, the cell sheets demonstrated 5-8 layers of cells piled on top of each other. Except for cells at the surface layer which were elongated, many cells in the interior were cuboidal in shape, with varying amounts of nuclear fragmentation and cell border irregularity scattered in a heterogeneous fashion (Fig. 15).

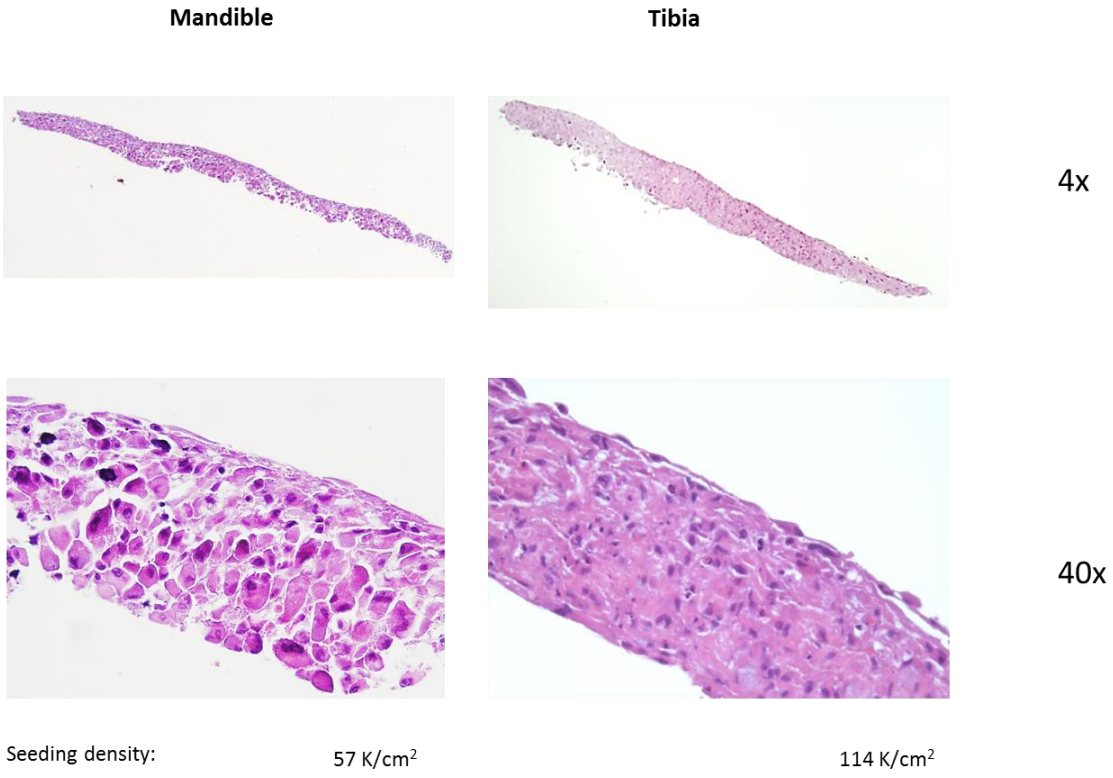

Fig. 15. H & E staining of mandibular and tibial BM-MSC cell sheets

CHAPTER 5

DISCUSSION AND CONLUSIONS

The purpose of this study was to compare BM-MSCs from the mandible to those from the tibia in a pig model. Specifically, we investigated their gene expression and some properties related to skeletal tissue regeneration including expression of mesenchymal stem cell markers, proliferation, osteogenic differentiation and ability to form scaffold-free cell sheets in vitro.

While bone marrow aspiration from pig tibiae or iliac crests has been routinely and consistently performed by many researchers, we established a method to aspirate bone marrow from the pig mandible for the first time. Based on experience from the four pigs used in this study, 10-18 mL bone marrow can be aspirated from the mandibular symphyseal region in four month old pigs through a single needle insertion. Although the abundance of bone marrow in the mandibular symphyseal region appears to be smaller than that from the tibia, 10-18 mL of bone marrow was adequate for subsequent isolation and expansion of BM-MSCs. Various studies have described isolating MSCs from a number of craniofacial sources including dental pulp and the periodontal ligament but few studies exist which describe harvesting stromal cells from craniofacial bone marrow. Due to the small size of craniofacial bones relative to long bones, the marrow volume is believed to be less abundant. Accordingly, previous investigators who attempted to isolate BM-MSCs from craniofacial bones have done so by rinsing trabecular bone fragments recovered at human third molar extractions sites[39] or by flushing bone marrow from the superior alveolar ridge through extraction sockets[45, 86] in rats. Therefore, we are the first group that directly aspirated appreciable volumes (11-18 mL) of bone marrow directly from the symphyseal area of juvenile porcine mandibles.

Through flow cytometry analysis, we confirmed that the stromal cells isolated from mandibular bone marrow are indeed mesenchymal stem cells (MSC). More specifically, both mandible and tibia BM-MSCs strongly expressed CD105/endoglin, CD90, and CD44 (surface markers of MSCs) and lacked expression of CD11b and CD45, surface markers expressed by hematopoetic stem cells (Fig. 3 and 4). These data corroborate findings from other investigators who isolated BM-MSCs from pig and human iliac crest and long bones and found them to be positive for CD105, CD44, and CD90[88-90], while negative for CD11b[91] and CD45[88, 90-92].

The ability of fast replication is an important property of MSCs needed for tissue engineering. Through a series of cell culturing and passaging experiments, we found that mandibular BM-MSCs proliferated significantly faster than tibial BM-MSCs. The mandibular BM-MSCs also outlasted the tibial BM-MSCs in maintaining a high proliferation rate through later passages. Our findings about BM-MSC proliferation are consistent with those reported by other groups[39, 45, 86], who phenotypically compared craniofacial and lower extremities BM-MSCs from humans or rats. Specifically, Akintoye's group evaluated the proliferative capacity of human BM-MSCs isolated from the mandible, maxilla, and iliac crest cells over the same time period (14 days) and showed that both maxillary and mandibular BM-MSCs proliferated faster than iliac crest BM-MSCs. They also reported delayed senescence of orofacial-derived BM-MSCs compared to iliac crest BM-MSCs. Similarly, rat mandibular BM-MSCs exhibited stronger proliferation and anti-apoptotic potentials as compared to long bone BM-MSCs[45, 86]. Morphologically, the iliac crest is a flat bone, while the tibia is a long bone. Anatomically, however, both the iliac crest and the tibia are bones of the lower extremity, and embryonically they share the same mesoderm origin. On the other hand, the jaws are craniofacial bones with both the mesoderm and cranial neural crest cells contributing to their embryonic development[87]. More importantly, cells expressing neural crest markers are known to be more pluripotent, a feature believed to contribute to the survival of MSCs in hypoxia after transplantation[93, 94] .

Therefore, despite the difference in research subjects between the present study and the Akintoye et al.'s and Dong's studies[39, 86], the combined data suggest that the cranial neural crest-derived BM-MSCs have a stronger proliferation potential than those from their mesodermal-derived counterparts in the limbs.

The ability of osteogenic differentiation is another important property of BM-MSCs for skeletal tissue engineering. In the present study, osteogenic capacity was compared by assessing ALP activity, an indicator for early osteogenic differentiation. Previous studies including those from our lab have evaluated osteogenic capacity of BM-MSCs in varied ways[38, 45, 95, 96]. Typically, the cultured cells were induced by supplementing the culturing media with ascorbic acid, dexamethasone, and β-glycerophosphate or using other commercially developed kits. As we previously found, however, even without osteogenic induction, the cultured BM-MSCs demonstrated a certain degree of ALP activity[38], suggesting that some of the replicated cells may be committed to the osteogenic lineage during *in vitro* expansion. This was confirmed in the current study, and the mandibular BM-MSCs appear to be stronger ALP producers than tibia BM-MSCs. We also found that these site-related differences were not changed by the addition of FGF-2. Previously we showed that when FGF-2 was used together with osteogenic media, osteogenic differentiation measured by ALP activity and Runx-2 expression was enhanced[38]. Other investigators have also shown that FGF-2 at concentrations as low as 1 ng/mL can increase ALP activity in human MSCs placed in osteogenic media[97]. The present data, however, seem to suggest that FGF-2 by itself does not act as an osteogenic inducer for either mandibular or tibial BM-MSCs. This may indicate that osteogenic inducers are required for FGF-2 to augment ALP activity in these cells and additional studies are warranted to evaluate this speculation. In a related study on rats, Aghaloo et al. and Dong et al. observed significantly greater ALP activity and osteocalcin expression in mandibular BM-MSCs than long bone BM-MSCs[45, 86]. The same trend of enhanced osteogenic potential of craniofacial-derived BM-MSCs was also reported in

humans using small marrow samples from third molar extraction sites[39]. Although we tested ALP activity without the addition of common osteogenic inducers while the other two groups did use osteogenic media, our findings are consistent with theirs. Combined, these data suggest that craniofacial BM-MSCs are likely advantageous to long bone BM-MSCs in terms of the ability of osteogenic differentiation. It is worth noting that our present data only reveal a small part of the osteogenic capacity of BM-MSCs as we only studied ALP activity. Future studies are needed to examine the expression of markers indicative of middle and late stage osteogenic differentiation such as osteopontin and osteocalcin, respectively[68, 98, 99] as well as type I collage and mineral production.

To assess whether this difference in proliferation and osteogenic differentiation is relevant to variation in gene expression, especially neural crest-related genes, we conducted a microarray assay. The results found that a total of 383 genes were significantly different between mandibular and tibial BM-MSCs (ANOVA test, $p < 0.05$), out of which 47 genes demonstrated >1.5 fold of differences, between the two locations. Generally gene expression with >2 fold of difference is considered as differentially expressed. Based on the 14 differentially expressed genes identified by the 2-fold criterion, one would quickly conclude the gene profiles between mandibular and tibial BM-MSCs are very similar. On one hand, as cells from both locations are BM-MSCs, it is not surprising that they have a high similarity in gene expression. On the other hand, however, it does not explain the phenotypical differences between the cells from the two sites, such as proliferation and differentiation as discussed above. Possible explanations become available when the microarray data were analyzed using more sophisticated methods. First, the hierarchical clustering was performed on the set of genes with at least 1.5-fold difference, which revealed a significant incongruence between the primary passage of BM-MSCs isolated from these two locations. Using the same cut-off criterion, DAVID analysis also categorized the gene profile into functional groups, which showed distinct differences between mandibular and tibial

BM-MSCs (Table 1). Specifically, mandibular BM-MSCs tended to be enriched in neurological processes and protein dimerization activity. In particular, two of the four genes involved in the protein dimerization activity, *BMP-4* and activating transcription factor (*ATF6*), are both related to cell survival[108, 109] and osteogenesis[100, 101]. *BMP-4* is also specifically a neural-crest gene, and was found critical for stem cell renewal and maintaining pluripotency. *Nestin* was another noteworthy upregulated neural crest marker in mandibular BM-MSCs, but only has a fold change of 1.23. It is also essential for cell proliferation and migration, while maintaining the stemness of the cell[102, 103]. In contrast, tibial BM-MSCs were enriched in cellular component lysosome, which is an organelle involved in the terminal steps of apoptosis[104]. These distinctive clusters , although categorized at a less stringent criterion (1.5 fold instead of 2 fold of difference), at least demonstrate a tendency that mandibular BM-MSCs have a higher chance of survival and osteogenic potential, while tibial BM-MSCs may be more prone to apoptosis, a finding that matches our proliferation and osteogenic differentiation data about these cells.

Next, when the highly abundant transcriptomes expressed were compared between BM-MSCs from the two locations, a distinct difference was also found. More specifically, with 75% of the highest expressed gene which have a log2 of 14.07 being compared, mandibular and tibial BM-MSCs were significantly enriched in angiogenesis and ossification, and other essential cellular functions such as cell motion and extracellular matrix organization (Table 1). In Monaco's microarray analysis comparing porcine BM-MSCs isolated from long bone and adipose tissue, they found that long bone BM-MSCs have higher angiogenic, osteogenic, migratory, and neurogenic capacity compared to adipose-derived MSCs[70]. Although the particular genes reported to be differentially expressed by Monaco et al. were not the same as ours, functional annotation analysis with DAVID found that the categories of genes of long bone BM-MSCs were similar between the two studies[70]. In our study, not only did the differentially expressed genes analysis demonstrate a tendency of higher neurogenic capacity in mandibular

BM-MSCs than long bone BM-MSCs in the highly abundant transcriptome analysis, mandibular BM-MSCs also demonstrated a tendency for stronger gene expression regulating endochondral ossification and skeletal muscle tissue development. This further explains the difference in osteogenic differentiation and implies that mandibular BM-MSCs are superior in bone regeneration to tibial BM-MSCs.

Undoubtedly, while microarray analysis is highly efficient in screening thousands of genes, precautions are warranted for the findings and interpretations. The number of subjects used in the present and the Monaco et al. study is relatively low, which may reduce statistical power and increases susceptibility to biases. Thus, additional tests are desired to confirm our gene expression microarray findings. Limited by the scope of this thesis project, however, we were not able to retest a large number of genes using RT-PCR that were found to be statistically differentially expressed between mandible and tibia BM-MSCs. As a result, we only further tested the expression of two genes known to be neural crest related, *BMP-4* and *nestin*, using RT-PCR tests. The results confirmed the trend reflected by the microarray assay. That is, both *BMP-4* and *nestin* tended to express more strongly in mandibular BM-MSCs than tibial BM-MSCs, although the net differences were less than one fold and did not reach statistical significance. Although *BMP-4* and *nestin* have been used as neural crest markers, their unique function in human development continues to be researched. *BMP-4* is essential for differentiation of mesoderm, including development of craniofacial and appendicular bone, and knockouts of this gene result in embryonic lethality[105]. *Nestin*, an intermediate filament protein, is expressed predominantly in rapidly dividing cells of developing and regenerating tissues and is understood to play an important role in central and peripheral nervous system development[106, 107]. For these reasons, it is understandable why some expression of these proteins is still recorded in tibial BM-MSCs even though are not of neural crest origin.

The last part of this study compared the ability of mandibular and tibial BM-MSCs in forming scaffold free cell sheets using thermo-responsive culturing dishes. Overall, mandibular BM-MSCs outperformed tibia BM-MSCs in two aspects: a lower seeding density is required to form single layer cell sheets and more cells remain viable on 3-layer cell sheets after 24 hours incubation based on live-dead cell staining. The reason for mandibular BM-MSCs to quickly form cell sheets may be partly attributable to their higher proliferation rate as discussed above. The reported seeding density for cell sheet formation varies greatly among studies[63, 68, 95]. In our study, we used higher seeding density than that used by some other investigators[68, 95], which resulted in a much shorter time to yield a complete cell sheet. More specifically, while others often cultured their cell sheets for as much as 10-13 days after initial seeding, we only needed two days. This not only eliminated the necessity to change the culturing media prior to harvest, but also improved the integrity of the cell sheets. In our trials where BM-MSC sheets were cultured longer, it was found that portions of the sheets began to detach prematurely in patchy, non-confluent patterns mainly at the outer edges of the sheet prior to harvest, likely because of temperature change at the edges of the culturing plates during media changes. Other investigators have discovered that adding vitamin c (V_c) in small doses (20-50 μg/mL) improves the sheet-forming ability of periodontal ligament stem cells (PDLSC) and this may be a promising method to improve the formation of these sheets in future trials[95].

As far as the cell viability is concerned, our H&E data are not consistent with the live/dead staining. Initial H&E evaluations of tibial and mandibular BM-MSC cell sheets were performed following live/dead staining and it was therefore reasoned that compromised cell viability, manifest by nuclear breakdown and poor cell boundaries, was due to UV damage associated with immunofluorescent microscopy. Later evaluation of cell sheets not exposed to UV light revealed that while the superficial layers appeared elongated with regular cell boundaries, there were still areas of overt necrosis throughout the interior. Although several

mechanisms may contribute to this finding, it is likely that cells in the deep layers of the sheet matrix experience hypoxic injury during the 24 hours following cell sheet stacking. Future studies will analyze the relationship among incubation time, oxygen concentration, and cell viability.

Finally, in the present study, all of the cell sheets were created using BM-MSCs that had been cultured exclusively in growth media alone. Later studies may also investigate the benefit of culturing BM-MSCs in media with exogenous osteogenic inducers. Based on related studies in which porcine-derived MSC cell sheets were wrapped around scaffold materials prior to transplantation into nude rats[65], the benefits of combining cell sheet technology with scaffold materials is also promising. It is anticipated that future studies will investigate the in vivo applications of using craniofacial-derived BM-MSCs sheets.

Limitations:

Although a sample size of four pigs is reasonable for studies of this nature, a greater number of subjects/samples would have increased the statistical power of our results. The number of surgeries required to acquire more samples required greater time and resources than were available. The significant cost of certain aspects of this study, specifically microarray technology, is a related limiting factor. Additionally, the amount of variability between subjects is sufficient to make it challenging reach statistical significance in some instances. As mentioned previously, our assessment of osteogenic capacity is limited in scope because we measured ALP prior to treating with osteogenic media. Greater understanding would be reached by evaluating ALP and other osteogenic markers after treating cells inducers such as dexamethasone, ascorbic acid, and β-glycerophosphate either by additional protein assays or quantitative PCR. Finally, the cell sheet experiments included in this study are in their preliminary stages and we are still testing the

feasibility of cell sheet stacking as well as analyzing the health of the cell sheets after they have been layered.

Conclusions:

This study establishes that BM-MSCs are readily obtainable from the pig mandible and demonstrates that MSCs from this location express a number of genes differently than those typically recovered from long bone marrow. Our findings not only support the concept of dissimilar embryologic origin between the two types of BM-MSCs, it validates that craniofacial-derived BM-MSCs have a distinct advantage in their capacity for bone regeneration due to higher proliferative ability and high propensity toward osteogenic differentiation. Our cell sheet-forming experiments further establish these mandibular BM-MSCs to be advantageous over tibial BM-MSCs due to their ability to form intact sheets with high cell viability using lower seeding densities. Future *in vivo* studies are warranted to test the combined efficacy of craniofacial-derived BM-MSCs and scaffold-free cell sheet technology for repair and regeneration of bony defects.

REFERENCES

1. Smith BT, Shum J, Wong M, Mikos AG, Young S. Bone Tissue Engineering Challenges in Oral & Maxillofacial Surgery. In: Bertassoni LE, Coelho, P.G., editor. Engineering Mineralized and Load Bearing Tissues (Advances in Experimental Medicine and Biology). Switzerland: Springer Intrnational; 2015. p. 276.
2. Proffit WR, Fields HW, Sarver DM. Contemporary Orthodontics: Elsevier Health Sciences; 2013.
3. Atwood DA. Reduction of residual ridges: a major oral disease entity. J Prosthet Dent 1971;26(3):266-79.
4. Schropp L, Wenzel A, Kostopoulos L, Karring T. Bone healing and soft tissue contour changes following single-tooth extraction: a clinical and radiographic 12-month prospective study. Int J Periodontics Restorative Dent 2003;23(4):313-23.
5. Larsson L, Decker AM, Nibali L, et al. Regenerative Medicine for Periodontal and Peri-implant Diseases. J Dent Res 2015.
6. Fretwurst T, Gad LM, Nelson K, Schmelzeisen R. Dentoalveolar reconstruction: modern approaches. Curr Opin Otolaryngol Head Neck Surg 2015;23(4):316-22.
7. Spin-Neto R, Stavropoulos A, Coletti FL, et al. Graft incorporation and implant osseointegration following the use of autologous and fresh-frozen allogeneic block bone grafts for lateral ridge augmentation. Clin Oral Implants Res 2014;25(2):226-33.
8. Barber HD, Betts NJ. Rehabilitation of maxillofacial trauma patients with dental implants. Implant Dent 1993;2(3):191-3.
9. Einhorn TA. The cell and molecular biology of fracture healing. Clin Orthop Rel Res 1998;355S:S7-S21.
10. Gamradt SC, Lieberman JR. Bone graft for revision hip arthroplasty: biology and future applications. Clin Orthop Relat Res 2003(417):183-94.
11. Jewer DD, Boyd JB, Manktelow RT, et al. Orofacial and mandibular reconstruction with the iliac crest free flap: a review of 60 cases and a new method of classification. Plast Reconstr Surg 1989;84(3):391-403; discussion 04-5.
12. Schoning H, Emshoff R. Primary temporary AO plate reconstruction of the mandible. Oral Surg Oral Med Oral Pathol Oral Radiol Endod 1998;86(6):667-72.
13. Urken ML, Bridger AG, Zur KB, Genden EM. The scapular osteofasciocutaneous flap: a 12-year experience. Arch Otolaryngol Head Neck Surg 2001;127(7):862-9.
14. Wei FC, Seah CS, Tsai YC, Liu SJ, Tsai MS. Fibula osteoseptocutaneous flap for reconstruction of composite mandibular defects. Plast Reconstr Surg 1994;93(2):294-304; discussion 05-6.
15. Goh BT, Lee S, Tideman H, Stoelinga PJ. Mandibular reconstruction in adults: a review. Int J Oral Maxillofac Surg 2008;37(7):597-605.
16. Krasny K, Kaminski A, Krasny M, et al. Clinical Use of Allogeneic Bone Granulates to Reconstruct Maxillary and Mandibular Alveolar Processes. Transplantation Proceedings 2011;43(8):3142-44.
17. Mardas N, Chadha V, Donos N. Alveolar ridge preservation with guided bone regeneration and a synthetic bone substitute or a bovine-derived xenograft: a randomized, controlled clinical trial. Clin Oral Implants Res 2010;21(7):688-98.

18. Chang EW, Lam SM, Karen M, Donlevy JL. Sliding genioplasty for correction of chin abnormalities. Arch Facial Plast Surg 2001;3(1):8-15.
19. Choe KS, Stucki-McCormick SU. Chin augmentation. Facial Plast Surg 2000;16(1):45-54.
20. Kumar P, Vinitha B, Fathima G. Bone grafts in dentistry. J Pharm Bioallied Sci 2013;5(Suppl 1):S125-7.
21. Van Sickels JE, Tiner BD. Cost of a genioplasty under deep intravenous sedation in a private office versus general anesthesia in an outpatient surgical center. J Oral Maxillofac Surg 1992;50(7):687-90.
22. Zins JE, Bruno J, Moreira-Gonzalez A, Bena J. Orthognathic surgery: is there a future? Plast Reconstr Surg 2005;116(5):1442-50; discussion 51-2.
23. Zins JE, Morrison CM, Gonzalez AM, Altus GD, Bena J. Follow-up: orthognathic surgery. Is there a future? A national survey. Plast Reconstr Surg 2008;122(2):555-62.
24. Eisele D, Smith R. Complications in Head and Neck Surgery. 2nd ed. Philadelphia: Mosby Elsevier; 2009.
25. Albrektsson T, Johansson C. Osteoinduction, osteoconduction and osseointegration. Eur Spine J 2001;10 Suppl 2:S96-101.
26. Younger EM, Chapman MW. Morbidity at bone graft donor sites. J Orthop Trauma 1989;3(3):192-5.
27. Banwart JC, Asher MA, Hassanein RS. Iliac crest bone graft harvest donor site morbidity. A statistical evaluation. Spine (Phila Pa 1976) 1995;20(9):1055-60.
28. Momoh AO, Yu P, Skoracki RJ, et al. A prospective cohort study of fibula free flap donor-site morbidity in 157 consecutive patients. Plast Reconstr Surg 2011;128(3):714-20.
29. Hekner DD, Abbink JH, van Es RJ, et al. Donor-site morbidity of the radial forearm free flap versus the ulnar forearm free flap. Plast Reconstr Surg 2013;132(2):387-93.
30. White JB, Dufresne CR. Management and avoidance of complications in chin augmentation. Aesthet Surg J 2011;31(6):634-42.
31. Hohl TH, Epker BN. Macrogenia: a study of treatment results, with surgical recommendations. Oral Surg Oral Med Oral Pathol 1976;41(5):545-67.
32. Grauer JN, Beiner JM, Kwon BK, Vaccaro AR. Bone graft alternatives for spinal fusion. BioDrugs 2003;17(6):391-4.
33. Vaccaro AR, Chiba K, Heller JG, et al. Bone grafting alternatives in spinal surgery. Spine J 2002;2(3):206-15.
34. Keating JF, McQueen MM. Substitutes for autologous bone graft in orthopaedic trauma. J Bone Joint Surg Br 2001;83(1):3-8.
35. Ross MH PW. Histology. 5th ed. Baltimore, MD: Lippincott Williams and Wilkins; 2006.
36. Service RF. Tissue engineers build new bone. Science 2000;289(5484):1498-500.
37. Kang HW, Lee SJ, Ko IK, et al. A 3D bioprinting system to produce human-scale tissue constructs with structural integrity. Nat Biotechnol 2016.
38. Sun Z, Tee BC, Kennedy KS, et al. Scaffold-based delivery of autologous mesenchymal stem cells for mandibular distraction osteogenesis: preliminary studies in a porcine model. PLoS One 2013;8(9):e74672.
39. Akintoye SO, Lam T, Shi S, et al. Skeletal site-specific characterization of orofacial and iliac crest human bone marrow stromal cells in same individuals. Bone 2006;38(6):758-68.
40. Gronthos S, Zannettino AC, Hay SJ, et al. Molecular and cellular characterisation of highly purified stromal stem cells derived from human bone marrow. J Cell Sci 2003;116(Pt 9):1827-35.

41. Owen M, Friedenstein AJ. Stromal stem cells: marrow-derived osteogenic precursors. Ciba Found Symp 1988;136:42-60.
42. Pereira RF, Halford KW, O'Hara MD, et al. Cultured adherent cells from marrow can serve as long-lasting precursor cells for bone, cartilage, and lung in irradiated mice. Proc Natl Acad Sci U S A 1995;92(11):4857-61.
43. Wagner W, Wein F, Seckinger A, et al. Comparative characteristics of mesenchymal stem cells from human bone marrow, adipose tissue, and umbilical cord blood. Exp Hematol 2005;33(11):1402-16.
44. Huang GT, Gronthos S, Shi S. Mesenchymal stem cells derived from dental tissues vs. those from other sources: their biology and role in regenerative medicine. J Dent Res 2009;88(9):792-806.
45. Aghaloo TL, Chaichanasakul T, Bezouglaia O, et al. Osteogenic potential of mandibular vs. long-bone marrow stromal cells. J Dent Res 2010;89(11):1293-8.
46. SF G. Developmental Biology. 6th ed. Sunderland, MA: Sinauer Associates, Inc.; 2000.
47. Sealfon SC, Chu TT. RNA and DNA microarrays. Methods Mol Biol 2011;671:3-34.
48. Leor J, Aboulafia-Etzion S, Dar A, et al. Bioengineered cardiac grafts: A new approach to repair the infarcted myocardium? Circulation 2000;102(19 Suppl 3):III56-61.
49. Zimmermann WH, Melnychenko I, Wasmeier G, et al. Engineered heart tissue grafts improve systolic and diastolic function in infarcted rat hearts. Nat Med 2006;12(4):452-8.
50. Shinoka T, Breuer C. Tissue-engineered blood vessels in pediatric cardiac surgery. Yale J Biol Med 2008;81(4):161-6.
51. Iwasa J, Engebretsen L, Shima Y, Ochi M. Clinical application of scaffolds for cartilage tissue engineering. Knee Surgery Sports Traumatology Arthroscopy 2009;17(6):561-77.
52. Lee K, Chan CK, Patil N, Goodman SB. Cell therapy for bone regeneration--bench to bedside. J Biomed Mater Res B Appl Biomater 2009;89(1):252-63.
53. Atala A, Lanza R, Thompson JA, Nerem R. Principles of Regenerative Medicine. 2nd ed. Burlington, MA: Academic Press / Elsevier; 2011.
54. Menasche P, Hagege AA, Scorsin M, et al. Myoblast transplantation for heart failure. Lancet 2001;357(9252):279-80.
55. Zhang M, Methot D, Poppa V, et al. Cardiomyocyte grafting for cardiac repair: graft cell death and anti-death strategies. J Mol Cell Cardiol 2001;33(5):907-21.
56. Suzuki K, Murtuza B, Beauchamp JR, et al. Dynamics and mediators of acute graft attrition after myoblast transplantation to the heart. FASEB J 2004;18(10):1153-5.
57. Kinoshita Y, Maeda H. Recent developments of functional scaffolds for craniomaxillofacial bone tissue engineering applications. ScientificWorldJournal 2013;2013:863157.
58. Langer R, Vacanti JP. Tissue engineering. Science 1993;260(5110):920-6.
59. Ma D, Ren L, Liu Y, et al. Engineering scaffold-free bone tissue using bone marrow stromal cell sheets. J Orthop Res 2010;28(5):697-702.
60. Haraguchi Y, Shimizu T, Sasagawa T, et al. Fabrication of functional three-dimensional tissues by stacking cell sheets in vitro. Nat Protoc 2012;7(5):850-8.
61. Yamada N, Okano T, Sakai H, et al. Thermoresponsive Polymeric Surfaces - Control of Attachment and Detachment of Cultured-Cells. Makromolekulare Chemie-Rapid Communications 1990;11(11):571-76.
62. Okano T, Yamada N, Sakai H, Sakurai Y. A novel recovery system for cultured cells using plasma-treated polystyrene dishes grafted with poly(N-isopropylacrylamide). J Biomed Mater Res 1993;27(10):1243-51.
63. Shimizu T, Yamato M, Isoi Y, et al. Fabrication of pulsatile cardiac tissue grafts using a novel 3-dimensional cell sheet manipulation technique and temperature-responsive cell culture surfaces. Circ Res 2002;90(3):e40.

64. Chen CH, Chang Y, Wang CC, et al. Construction and characterization of fragmented mesenchymal-stem-cell sheets for intramuscular injection. Biomaterials 2007;28(31):4643-51.
65. Zhou Y, Chen F, Ho ST, et al. Combined marrow stromal cell-sheet techniques and high-strength biodegradable composite scaffolds for engineered functional bone grafts. Biomaterials 2007;28(5):814-24.
66. Freshney RI. Culture of animal cells: a manual of basic technique. 3rd ed. New York, NY: Wiley-Liss; 1994.
67. Memon IA, Sawa Y, Fukushima N, et al. Repair of impaired myocardium by means of implantation of engineered autologous myoblast sheets. J Thorac Cardiovasc Surg 2005;130(5):1333-41.
68. Uchiyama H, Yamato M, Sasaki R, et al. In vivo 3D analysis with micro-computed tomography of rat calvaria bone regeneration using periosteal cell sheets fabricated on temperature-responsive culture dishes. J Tissue Eng Regen Med 2011;5(6):483-90.
69. Liu Y, Ming L, Luo H, et al. Integration of a calcined bovine bone and BMSC-sheet 3D scaffold and the promotion of bone regeneration in large defects. Biomaterials 2013;34(38):9998-10006.
70. Monaco E, Bionaz M, Rodriguez-Zas S, Hurley WL, Wheeler MB. Transcriptomics comparison between porcine adipose and bone marrow mesenchymal stem cells during in vitro osteogenic and adipogenic differentiation. PLoS One 2012;7(3):e32481.
71. Phillips RW, Tumbleson ME. Swine in Biomedical Research. In: Tumbleson ME, editor. Models, Swine in biomedical research. New Yord, NY: Plenum Press; 1986.
72. Chang SC, Wei FC, Chuang H, et al. Ex vivo gene therapy in autologous critical-size craniofacial bone regeneration. Plast Reconstr Surg 2003;112(7):1841-50.
73. von Wilmowsky C, Stockmann P, Metzler P, et al. Establishment of a streptozotocin-induced diabetic domestic pig model and a systematic evaluation of pathological changes in the hard and soft tissue over a 12-month period. Clin Oral Implants Res 2010;21(7):709-17.
74. Herring SW. The dynamics of mastication in pigs. Arch Oral Biol 1976;21:473-80.
75. Bianco P, Kuznetsov SA, Riminucci M, Gehron Robey P. Postnatal skeletal stem cells. Methods Enzymol 2006;419:117-48.
76. Bauer TW, Muschler GF. Bone graft materials. An overview of the basic science. Clin Orthop Relat Res 2000(371):10-27.
77. Friedenstein AJ, Gorskaja JF, Kulagina NN. Fibroblast precursors in normal and irradiated mouse hematopoietic organs. Exp Hematol 1976;4(5):267-74.
78. Knight MN, Hankenson KD. Mesenchymal Stem Cells in Bone Regeneration. Adv Wound Care (New Rochelle) 2013;2(6):306-16.
79. Kaigler D, Pagni G, Park CH, et al. Stem cell therapy for craniofacial bone regeneration: a randomized, controlled feasibility trial. Cell Transplant 2013;22(5):767-77.
80. Soltan M, Smiler D, Prasad HS, Rohrer MD. Bone block allograft impregnated with bone marrow aspirate. Implant Dent 2007;16(4):329-39.
81. Kawaguchi H, Hirachi A, Hasegawa N, et al. Enhancement of periodontal tissue regeneration by transplantation of bone marrow mesenchymal stem cells. J Periodontol 2004;75(9):1281-7.
82. Cerruti HF, Kerkis I, Kerkis A, et al. Allogenous bone grafts improved by bone marrow stem cells and platelet growth factors: Clinical case reports. Artificial Organs 2007;31(4):268-73.
83. Xie J, Han Z, Naito M, et al. Articular cartilage tissue engineering based on a mechano-active scaffold made of poly(L-lactide-co-epsilon-caprolactone): In vivo performance in adult rabbits. J Biomed Mater Res B Appl Biomater 2010;94(1):80-8.

84. Li H, Yan F, Lei L, Li Y, Xiao Y. Application of autologous cryopreserved bone marrow mesenchymal stem cells for periodontal regeneration in dogs. Cells Tiss. Org. 2009;190(2):94-101.
85. Marei MK, Nouh SR, Saad MM, Ismail NS. Preservation and regeneration of alveolar bone by tissue-engineered implants. Tissue Eng 2005;11(5-6):751-67.
86. Dong W, Ge J, Zhang P, et al. Phenotypic characterization of craniofacial bone marrow stromal cells: unique properties of enhanced osteogenesis, cell recruitment, autophagy, and apoptosis resistance. Cell Tissue Res 2014;358(1):165-75.
87. Chai Y, Jiang X, Ito Y, et al. Fate of the mammalian cranial neural crest during tooth and mandibular morphogenesis. Dev 2000;127(8):1671-9.
88. Noort WA, Oerlemans MI, Rozemuller H, et al. Human versus porcine mesenchymal stromal cells: phenotype, differentiation potential, immunomodulation and cardiac improvement after transplantation. J Cell Mol Med 2012;16(8):1827-39.
89. Bruckner S, Tautenhahn HM, Winkler S, et al. A fat option for the pig: hepatocytic differentiated mesenchymal stem cells for translational research. Exp Cell Res 2014;321(2):267-75.
90. Bruckner S, Tautenhahn HM, Winkler S, et al. Isolation and hepatocyte differentiation of mesenchymal stem cells from porcine bone marrow--"surgical waste" as a novel MSC source. Transplant Proc 2013;45(5):2056-8.
91. Colter DC, Class R, DiGirolamo CM, Prockop DJ. Rapid expansion of recycling stem cells in cultures of plastic-adherent cells from human bone marrow. Proc Natl Acad Sci U S A 2000;97(7):3213-8.
92. Pittenger MF, Mackay AM, Beck SC, et al. Multilineage potential of adult human mesenchymal stem cells. Science 1999;284(5411):143-7.
93. Millman JR, Tan JH, Colton CK. The effects of low oxygen on self-renewal and differentiation of embryonic stem cells. Curr Opin Organ Transplant 2009;14(6):694-700.
94. Pan H, Cai N, Li M, Liu GH, Izpisua Belmonte JC. Autophagic control of cell 'stemness'. EMBO Mol Med 2013;5(3):327-31.
95. Wei F, Qu C, Song T, et al. Vitamin C treatment promotes mesenchymal stem cell sheet formation and tissue regeneration by elevating telomerase activity. J Cell Physiol 2012;227(9):3216-24.
96. Fiorentini E, Granchi D, Leonardi E, Baldini N, Ciapetti G. Effects of osteogenic differentiation inducers on in vitro expanded adult mesenchymal stromal cells. Int J Artif Organs 2011;34(10):998-1011.
97. Ito T, Sawada R, Fujiwara Y, Tsuchiya T. FGF-2 increases osteogenic and chondrogenic differentiation potentials of human mesenchymal stem cells by inactivation of TGF-beta signaling. Cytotechnology 2008;56(1):1-7.
98. Weinreb M, Shinar D, Rodan GA. Different pattern of alkaline phosphatase, osteopontin, and osteocalcin expression in developing rat bone visualized by in situ hybridization. J Bone Miner Res 1990;5(8):831-42.
99. Yoshikawa T, Ohgushi H, Okumura M, et al. Biochemical and histological sequences of membranous ossification in ectopic site. Calcif Tissue Int 1992;50(2):184-8.
100. Valcourt U, Moustakas A. BMP Signaling in Osteogenesis, Bone Remodeling and Repair. European Journal of Trauma 2005;31(5):464-79.
101. Jang WG, Kim EJ, Kim DK, et al. BMP2 protein regulates osteocalcin expression via Runx2-mediated Atf6 gene transcription. J Biol Chem 2012;287(2):905-15.
102. Suzuki S, Namiki J, Shibata S, Mastuzaki Y, Okano H. The neural stem/progenitor cell marker nestin is expressed in proliferative endothelial cells, but not in mature vasculature. J Histochem Cytochem 2010;58(8):721-30.
103. Xue XJ, Yuan XB. Nestin is essential for mitogen-stimulated proliferation of neural progenitor cells. Molecular and Cellular Neuroscience 2010;45(1):26-36.

104. Ivanova S, Repnik U, Bojic L, et al. Lysosomes in apoptosis. Programmed Cell Death, General Principles for Studying Cell Death, Pt A 2008;442:183-99.
105. Wang RN, Green J, Wang Z, et al. Bone Morphogenetic Protein (BMP) signaling in development and human diseases. Genes Dis 2014;1(1):87-105.
106. Michalczyk K, Ziman M. Nestin structure and predicted function in cellular cytoskeletal organisation. Histol Histopathol 2005;20(2):665-71.
107. Chen J, Boyle S, Zhao M, et al. Differential expression of the intermediate filament protein nestin during renal development and its localization in adult podocytes. J Am Soc Nephrol 2006;17(5):1283-91.
108. Teodoro T, Odisho T, Sidorova E, Volchuk A. Pancreatic beta-cells depend on basal expression of active ATF6alpha-p50 for cell survival even under nonstress conditions. Am J Physiol Cell Physiol 2012;302(7):C992-1003.
109. Ueki Y, Reh TA. Activation of BMP-Smad1/5/8 signaling promotes survival of retinal ganglion cells after damage in vivo. PLoS One 2012;7(6):e38690.